EUROPEAN ORGANIZATION FOR NUCLEAR RESEARCH (CERN)

CERN-EP/2016-111
2018/04/28

CMS-SUS-15-007

Search for supersymmetry in pp collisions at $\sqrt{s} = 13\,\text{TeV}$ in the single-lepton final state using the sum of masses of large-radius jets

The CMS Collaboration*

Abstract

Results are reported from a search for supersymmetric particles in proton-proton collisions in the final state with a single, high transverse momentum lepton; multiple jets, including at least one b-tagged jet; and large missing transverse momentum. The data sample corresponds to an integrated luminosity of $2.3\,\text{fb}^{-1}$ at $\sqrt{s} = 13\,\text{TeV}$, recorded by the CMS experiment at the LHC. The search focuses on processes leading to high jet multiplicities, such as gluino pair production with $\widetilde{\text{g}} \to \text{t}\bar{\text{t}}\widetilde{\chi}_1^0$. The quantity M_J, defined as the sum of the masses of the large-radius jets in the event, is used in conjunction with other kinematic variables to provide discrimination between signal and background and as a key part of the background estimation method. The observed event yields in the signal regions in data are consistent with those expected for standard model backgrounds, estimated from control regions in data. Exclusion limits are obtained for a simplified model corresponding to gluino pair production with three-body decays into top quarks and neutralinos. Gluinos with a mass below 1600 GeV are excluded at a 95% confidence level for scenarios with low $\widetilde{\chi}_1^0$ mass, and neutralinos with a mass below 800 GeV are excluded for a gluino mass of about 1300 GeV. For models with two-body gluino decays producing on-shell top squarks, the excluded region is only weakly sensitive to the top squark mass.

Published in the Journal of High Energy Physics as doi:10.1007/JHEP08(2016)122.

*See Appendix A for the list of collaboration members

1 Introduction

Supersymmetry (SUSY) [1–8] is an extension of the standard model (SM) of particle physics that is motivated by several considerations, including the gauge hierarchy problem [9–14], the existence of astrophysical dark matter [15–17], and the possibility of gauge coupling constant unification at high energy [18–22]. In SUSY models, each SM particle has a corresponding supersymmetric partner (or partners) whose spin differs by one-half, such that fermions are mapped to bosons and vice versa. Gauge quantum numbers are preserved by this symmetry, and to preserve degrees of freedom, a SM spin-1/2 Dirac particle, such as the top quark, has two spin-0 partners, the top squarks. The SUSY partner of the (spin-1) gluon, the massless mediator of the strong interactions in the SM, is the spin-1/2 gluino. In R-parity–conserving models [23, 24], SUSY particles are produced in pairs, and the lightest supersymmetric particle (LSP) is stable. If the LSP is the lightest neutralino ($\widetilde{\chi}_1^0$), an electrically neutral mixture of the SUSY partners of the neutral electroweak gauge and Higgs bosons, then it has weak interactions only and can in principle account for some or all of the dark matter.

The gauge hierarchy problem has become more urgent with the discovery of the Higgs boson [25–30]. Although the SM is conceptually complete, the Higgs boson mass, together with the electroweak scale, is unstable against enormous corrections from loop processes, which pull the Higgs mass to the cutoff scale of the theory, for example, the Planck scale. This outcome can be avoided within the framework of the SM only with extreme fine tuning of the bare Higgs mass parameter, a situation that is regarded as unnatural, although not excluded. This problem suggests that additional symmetries and associated degrees of freedom may be present that ameliorate these effects. So-called natural SUSY models [31–34], in which sufficiently light SUSY partners are present, are a major focus of current new physics searches at the CERN LHC. In natural models, several of the SUSY partners are constrained to be light [33]: both top squarks, $\widetilde{\mathrm{t}}_L$ and $\widetilde{\mathrm{t}}_R$, which have the same electroweak couplings as the left- (L) and right- (R) handed top quarks, respectively; the bottom squark with L-handed couplings ($\widetilde{\mathrm{b}}_L$); the gluino ($\widetilde{\mathrm{g}}$); and the Higgsinos ($\widetilde{\mathrm{h}}$). While the gluino mass is not constrained by naturalness considerations as strongly as that of the lighter top squark mass eigenstate, $\widetilde{\mathrm{t}}_1$, the cross section for gluino pair production is substantially larger than that for top squark pair production, for a given mass. As a consequence, the two types of searches can have comparable sensitivity to these models. Both types of searches are currently of intense interest, and CMS and ATLAS data taken at $\sqrt{s} = 8$ TeV have provided significant constraints [35] on natural SUSY scenarios.

This study uses the first LHC proton-proton collision data taken by the CMS experiment at $\sqrt{s} = 13$ TeV to search for gluino pair production. Searches targeting this process in the single-lepton final state using 8 TeV data have been performed by both ATLAS [36, 37] and CMS [38]. For $m_{\widetilde{\mathrm{g}}} = 1.5$ TeV, somewhat above the highest gluino masses excluded at $\sqrt{s} = 8$ TeV, the cross section for gluino pair production increases dramatically with center-of-mass energy, from about 0.4 fb at $\sqrt{s} = 8$ TeV to about 14 fb at $\sqrt{s} = 13$ TeV [39]. In contrast, the cross section for the dominant background, $\mathrm{t\bar{t}}$ production, increases much more slowly, from about 248 pb at $\sqrt{s} = 8$ TeV to 816 pb at $\sqrt{s} = 13$ TeV [40]. As a consequence, the sensitivity of this search can be significantly extended with respect to searches performed at $\sqrt{s} = 8$ TeV, even though the 13 TeV data sample has an integrated luminosity of only 2.3 fb^{-1}, roughly one-tenth of that acquired at 8 TeV.

The search targets gluino pair production with $\widetilde{\mathrm{g}} \to \mathrm{t\bar{t}}\widetilde{\chi}_1^0$, which arises from $\widetilde{\mathrm{g}} \to \widetilde{\mathrm{t}}_1\bar{\mathrm{t}}$, where the top squark is produced either on or off mass shell. The off-mass-shell scenario is shown in Fig. 1 (left) and is often designated T1tttt [41] in simplified model scenarios [42–44]. Results are also obtained for scenarios with on-shell top squark masses. This scenario is shown in

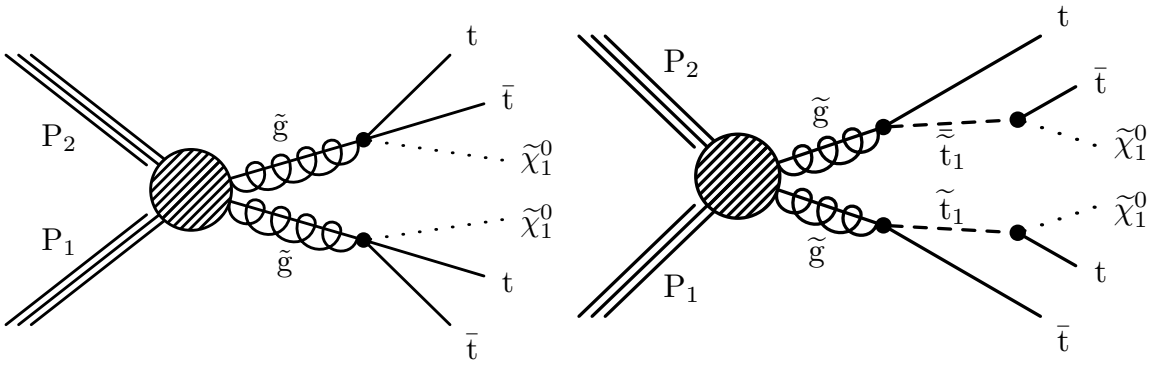

Figure 1: Gluino pair production and decay for the simplified models T1tttt (left) and T5tttt (right). In T1tttt, the gluino undergoes three-body decay $\widetilde{g} \to t\bar{t}\widetilde{\chi}_1^0$ via a virtual intermediate top squark. In T5tttt, the gluino decays via the sequential two-body process $\widetilde{g} \to \widetilde{t}_1\bar{t}$, $\widetilde{t}_1 \to t\widetilde{\chi}_1^0$. Because gluinos are Majorana particles, each one can decay to $\widetilde{t}_1\bar{t}$ and to the charge conjugate final state $\bar{\widetilde{t}}_1 t$.

Fig. 1 (right) and will be denoted by T5tttt. (For this scenario, the small contribution from the direct production of top squark pairs is also taken into account.) Regardless of whether the top squark is produced on or off mass shell, the final state is characterized by a large number of jets, four of which are b jets from top quark decays. Depending on the decay modes of the accompanying W bosons, a range of lepton multiplicities is possible; we focus here on the single-lepton final state, where the lepton is either an electron or a muon. Because the two neutralinos ($\widetilde{\chi}_1^0$) are undetected, their production in SUSY events typically gives rise to a large amount of missing (unobserved) momentum, whose value in the direction transverse to the beam axis can be inferred from the momenta of the observed particles. The missing transverse momentum, $\vec{p}_{\mathrm{T}}^{\,\mathrm{miss}}$, is a key element of searches for R-parity-conserving SUSY, and its magnitude is denoted by $E_{\mathrm{T}}^{\mathrm{miss}}$.

A challenge in performing searches for SUSY particles is obtaining sufficient sensitivity to the signal, while at the same time understanding the background contribution from SM processes in a robust manner. This analysis is designed such that the background in the signal regions arises largely from a single process, dilepton $t\bar{t}$ production, in which both W bosons from $t \to bW^+$ decay leptonically, but only one lepton satisfies the criteria associated with identification, the minimum transverse momentum (p_{T}) requirement, and isolation from other energy in the event. The search signature is characterized not only by the presence of high-p_{T} jets and b-tagged jets, an isolated high-p_{T} lepton, and large $E_{\mathrm{T}}^{\mathrm{miss}}$, but also by additional kinematic variables. Apart from resolution effects, the transverse mass of the lepton + $\vec{p}_{\mathrm{T}}^{\,\mathrm{miss}}$ system, m_{T}, is bounded above by m_{W} for events with a single leptonically decaying W, and this variable is very effective in suppressing the otherwise dominant single-lepton $t\bar{t}$ background. The quantity M_J, the scalar sum of the masses of large-radius jets, is used both to characterize the mass and energy scale of the event, providing discrimination between signal and background, and as a key part of the background estimation. A property of M_J exploited in this analysis is that, for the dominant background, this variable is nearly uncorrelated with m_{T}. Because of the absence of correlation between M_J and m_{T}, the background shape at high m_{T}, including the signal region, can be measured to a very good approximation using a low-m_{T} control sample. The quantity M_J was first discussed in phenomenological studies, for example, in Refs. [45–47]. Similar variables have been used by ATLAS for SUSY searches in all-hadronic final states using 8 TeV data [48, 49]. We have presented studies of basic M_J properties and performance using early 13 TeV data [50].

This paper is organized as follows. Section 2 gives a brief overview of the CMS detector. Section 3 discusses the simulated event samples used in the analysis. The event reconstruction is discussed in Section 4, while Section 5 describes the trigger and event selection. Section 6 presents the methodology used to predict the SM background from the event yields in control regions in data. The associated systematic uncertainties are also discussed. The event yields observed in the signal regions are presented in Section 7. These yields are compared with background predictions and used to obtain exclusion regions for the gluino pair production models shown in Fig. 1. Finally, Section 8 presents a summary of the methodology and the results.

2 Detector

The central feature of the CMS detector is a superconducting solenoid of 6 m internal diameter, providing a magnetic field of 3.8 T. Within the solenoid volume are the tracking and calorimeter systems. The tracking system, composed of silicon-pixel and silicon-strip detectors, measures charged particle trajectories within the pseudorapidity range $|\eta| < 2.5$, where $\eta \equiv -\ln[\tan(\theta/2)]$ and θ is the polar angle of the trajectory of the particle with respect to the counterclockwise proton beam direction. A lead tungstate crystal electromagnetic calorimeter (ECAL), and a brass and scintillator hadron calorimeter (HCAL), each composed of a barrel and two endcap sections, provide energy measurements up to $|\eta| = 3$. Forward calorimeters extend the pseudorapidity coverage provided by the barrel and endcap detectors up to $|\eta| = 5$. Muons are identified and measured within the range $|\eta| < 2.4$ by gas-ionization detectors embedded in the steel magnetic flux-return yoke outside the solenoid. The detector is nearly hermetic, permitting the accurate measurement of $\vec{p}_{\mathrm{T}}^{\,\mathrm{miss}}$. A more detailed description of the CMS detector, together with a definition of the coordinate system used and the relevant kinematic variables, is given in Ref. [51].

3 Simulated event samples

The analysis makes use of several simulated event samples for modeling the SM background and signal processes. While the background estimation in the analysis is performed largely from control samples in the data, simulated event samples provide correction factors, typically near unity. The equivalent integrated luminosity of the simulated event samples is at least six times that of the data, and at least 100 times that of the data in the case of $\mathrm{t\bar{t}}$ and signal processes.

The production of $\mathrm{t\bar{t}}$+jets, W+jets, Z+jets, and QCD multijet events is simulated with the Monte Carlo (MC) generator MADGRAPH5_AMC@NLO 2.2.2 [52] in leading-order (LO) mode. Single top quark events are modeled at next-to-leading order (NLO) with MADGRAPH5_AMC@NLO for the s-channel and POWHEG v2 [53, 54] for the t-channel and W-associated production. Additional small backgrounds, such as $\mathrm{t\bar{t}}$ production in association with bosons, diboson processes, and $\mathrm{t\bar{t}t\bar{t}}$ are similarly produced at NLO with either MADGRAPH5_AMC@NLO or POWHEG. All events are generated using the NNPDF 3.0 [55] set of parton distribution functions (PDF). Parton showering and fragmentation are performed with the PYTHIA 8.205 [56] generator with the underlying event model based on the CUETP8M1 tune detailed in Ref. [57]. The detector simulation is performed with GEANT4 [58]. The cross sections used to scale simulated event yields are based on the highest order calculation available. For $\mathrm{t\bar{t}}$, in addition to using the next-to-next-to-leading order + next-to-next-to-leading logarithmic cross section calculation [40], the modeling of the event kinematics is improved by reweighting the top quark p_{T} spectrum to match the data [59], keeping the overall normalization fixed.

Signal events for the T1tttt and T5tttt simplified models are generated in a manner similar to

that for the SM backgrounds, with the MADGRAPH5_AMC@NLO 2.2.2 generator in LO mode using the NNPDF 3.0 PDF set and followed with PYTHIA 8.205 for showering and fragmentation. The detector simulation is performed with the CMS fast simulation package [60] with scale factors applied to account for any differences with respect to the full simulation used for backgrounds. Event samples are generated for a representative set of model scenarios by scanning over the relevant mass ranges for the $\tilde{g}$ and $\tilde{\chi}_1^0$, and the yields are normalized to the NLO + next-to-leading-logarithmic cross section [39, 61–64].

Throughout this paper, two T1tttt benchmark models are used to illustrate typical signal behavior. The T1tttt(1500,100) model, with masses $m_{\tilde{g}} = 1500\,\text{GeV}$ and $m_{\tilde{\chi}_1^0} = 100\,\text{GeV}$, corresponds to a scenario with a large mass splitting (referred to as non-compressed, or NC) between the gluino and the neutralino. This mass combination probes the sensitivity of the analysis to a low cross section (14 fb) process that has a hard E_T^miss spectrum, which results in a relatively high signal efficiency. The T1tttt(1200,800) model, with masses $m_{\tilde{g}} = 1200\,\text{GeV}$ and $m_{\tilde{\chi}_1^0} = 800\,\text{GeV}$, corresponds to a scenario with a small mass splitting (referred to as compressed, or C) between the gluino and the neutralino. Here the cross section is much higher (86 fb) because the gluino mass is lower than for the T1tttt(1500,100) model, but the sensitivity suffers from a low signal efficiency due to the soft E_T^miss spectrum.

Finally, to model the presence of additional proton-proton collisions from the same or adjacent beam crossing as the primary hard-scattering process ("pileup" interactions), the simulated events are overlaid with multiple minimum bias events, which are also generated with the PYTHIA 8.205 generator with the underlying event model based on the CUETP8M1 tune. The distribution of the number of overlaid minimum bias events is broad and peaks in the range 10–15.

4 Event reconstruction

The reconstruction of physics objects in an event proceeds from the candidate particles identified by the particle-flow (PF) algorithm [65, 66], which uses information from the tracker, calorimeters, and muon systems to identify the candidates as charged or neutral hadrons, photons, electrons, or muons. Charged particle tracks are required to originate from the event primary vertex (PV), defined as the reconstructed vertex, located within 24 cm (2 cm) of the center of the detector in the direction along (perpendicular to) the beam axis, that has the highest value of p_T^2 summed over the associated charged particle tracks.

The charged PF candidates associated with the PV and the neutral PF candidates are clustered into jets using the anti-k_T algorithm [67] with distance parameter $R = 0.4$, as implemented in the FASTJET package [68]. The estimated pileup contribution to the jet p_T from neutral PF candidates is removed with a correction based on the area of the jet and the average energy density of the event [69]. The jet energy is calibrated using p_T- and η-dependent corrections; the resulting calibrated jet is required to satisfy $p_\text{T} > 30\,\text{GeV}$ and $|\eta| \leq 2.4$. Each jet must also meet loose identification requirements [70] to suppress, for example, calorimeter noise. Finally, jets that have PF constituents matched to an isolated lepton, as defined below, are removed from the jet collection.

A subset of the jets are "tagged" as originating from b quarks using the combined secondary vertex (CSV) algorithm [71, 72]. For the CSV medium working point chosen for this analysis, the signal efficiency for b jets in the range $p_\text{T} = 30$ to 50 GeV is 60–67% (51–57%) in the barrel (endcap), increasing with p_T. Above $p_\text{T} \approx 150\,\text{GeV}$ the b tagging efficiency decreases. The probability to misidentify jets arising from c quarks is 13–15% (11–13%) in the barrel (endcap),

while the misidentification probability for light-flavor quarks or gluons is 1–2%.

Throughout this paper, quantities related to the number of jets (N_{jets}) or to the number of b-tagged jets (N_{b}) are based only on small-R jets, not on the large-R jets discussed below.

Electrons are reconstructed by associating a charged particle track with an ECAL supercluster [73]. The resulting candidate electrons are required to have $p_{\text{T}} > 20\,\text{GeV}$ and $|\eta| < 2.5$, and to satisfy identification criteria designed to remove light-parton jets, photon conversions, and electrons from heavy flavor hadron decays. Muons are reconstructed by associating tracks in the muon system with those found in the silicon tracker [74]. Muon candidates are required to satisfy $p_{\text{T}} > 20\,\text{GeV}$ and $|\eta| < 2.4$.

To preferentially select leptons that originate in the decay of W bosons, leptons are required to be isolated from other PF candidates. Isolation is quantified using an optimized version of the "mini-isolation" variable originally suggested in Ref. [75], in which the transverse energy of the particles within a cone in η-ϕ space surrounding the lepton momentum vector is computed using a cone size that scales as $1/p_{\text{T}}^{\ell}$, where p_{T}^{ℓ} is the transverse momentum of the lepton. In this analysis, mini-isolation, $I_{\text{mini}}^{\text{rel}}$, is defined as the transverse energy of particles in a cone of radius $R^{\text{mini-iso}}$ around the lepton, divided by p_{T}^{ℓ}. The transverse energy is computed as the scalar sum of the p_{T} values of the charged hadrons from the PV, neutral hadrons, and photons. The neutral hadron and photon contributions to this sum are corrected for pileup. The cone radius $R^{\text{mini-iso}}$ varies with the p_{T}^{ℓ} according to

$$R^{\text{mini-iso}} = \begin{cases} 0.2, & p_{\text{T}}^{\ell} \leq 50\,\text{GeV} \\ (10\,\text{GeV})/p_{\text{T}}^{\ell}, & p_{\text{T}}^{\ell} \in (50\,\text{GeV}, 200\,\text{GeV}) \\ 0.05, & p_{\text{T}}^{\ell} \geq 200\,\text{GeV}. \end{cases} \tag{1}$$

The $1/p_{\text{T}}^{\ell}$ dependence is motivated by considering a two-body decay of a massive parent particle with mass M and large p_{T}, for which the angular separation of the daughter particles is roughly $\Delta R_{\text{daughters}} \approx 2M/p_{\text{T}}$. The p_{T}-dependent cone size reduces the rate of accidental overlaps between the lepton and jets in high-multiplicity or highly Lorentz-boosted events, particularly overlaps between b jets and leptons originating from a boosted top quark. The cone remains large enough to contain b-hadron decay products for non-prompt leptons across a range of p_{T}^{ℓ} values. Muons (electrons) must satisfy $I_{\text{mini}}^{\text{rel}} < 0.2\,(0.1)$. The combined efficiency for the electron reconstruction and isolation requirements is about 50% at a p_{T}^{ℓ} of 20 GeV, increasing to 65% at 50 GeV and reaching a plateau of 80% above 200 GeV. The combined reconstruction and isolation efficiencies for muons are about 70% at a p_{T}^{ℓ} of 20 GeV, increasing to 80% at 50 GeV and reaching a plateau of 95% at 200 GeV.

We cluster $R = 0.4$ ("small-R") jets and the isolated leptons into $R = 1.2$ ("large-R") jets using the anti-k_{T} algorithm. The mass of the large-R jets retains angular information about the clustered objects, as well as their p_{T} and multiplicity. Clustering small-R jets instead of PF candidates incorporates the jet pileup corrections, thereby reducing the dependence of the mass on pileup. The variable M_J is defined as the sum of all large-R jet masses:

$$M_J = \sum_{J_i = \text{large-}R\text{ jets}} m(J_i). \tag{2}$$

The technique of clustering small-R jets into large-R jets has been used previously by ATLAS in, for example, Ref. [76]. Leptons are included in the large-R jets to include the full kinematics of the event, and the choice $R = 1.2$ optimizes the background rejection power of M_J while retaining signal efficiency. Larger distance parameters were found to offer no significant addi-

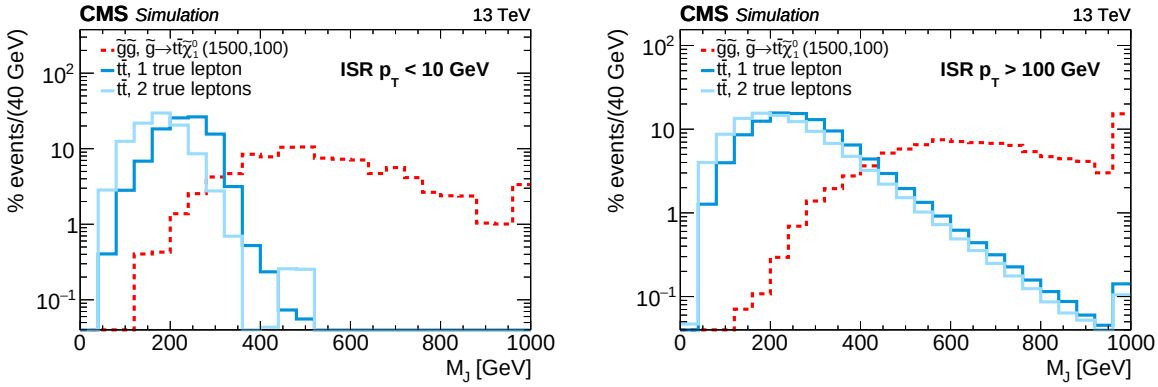

Figure 2: Distributions of M_J, normalized to the same area, from simulated event samples with a small ISR contribution (left) and a significant ISR contribution (right). These components are defined according to whether the p_T of the $t\bar{t}$ system (or, in the case of signal events, that of the $\tilde{g}\tilde{g}$ system) is <10 GeV or >100 GeV, respectively. The T1tttt(NC) signal model (dashed red line), is described in Section 3; the first model parameter in parentheses corresponds to $m_{\tilde{g}}$ and the second to $m_{\tilde{\chi}_1^0}$, both in units of GeV. The events satisfy the requirements $E_T^{miss} > 200$ GeV and $H_T > 500$ GeV and have at least one reconstructed lepton.

tional discriminating power, while smaller parameters decrease the background rejection up to a factor of two for models with small mass splittings between the gluino and neutralino.

For $t\bar{t}$ events with a small contribution from initial-state radiation (ISR), the M_J distribution has an approximate cutoff at twice the mass of the top quark, as shown in Fig. 2 (left). In contrast, the M_J distribution for signal events extends to larger values. The presence of a significant amount of ISR generates a high-M_J tail in the $t\bar{t}$ background, as shown in Fig. 2 (right).

The missing transverse energy, E_T^{miss}, is given by the magnitude of $\vec{p}_T^{miss}$, the negative vector sum of the transverse momenta of all PF candidates [65, 66]. Correspondence to the true undetectable energy in the event is improved by replacing the contribution of the PF candidates associated with a jet by the calibrated four-momentum of that jet. To separate backgrounds characterized by the presence of a single W boson decaying leptonically but without any other source of missing energy, the lepton and the E_T^{miss} are combined to obtain the transverse mass, m_T, defined as:

$$m_T = \sqrt{2p_T^{\ell} E_T^{miss}[1 - \cos(\Delta\phi_{\ell,\vec{p}_T^{miss}})]}, \quad (3)$$

where $\Delta\phi_{\ell,\vec{p}_T^{miss}}$ is the difference between the azimuthal angles of the lepton momentum vector and the missing momentum vector, $\vec{p}_T^{miss}$. Finally, we define the quantity H_T as the scalar sum of the transverse momenta of all the small-R jets passing the selection.

5 Trigger and event selection

The data sample used in this analysis was obtained with triggers that require $H_T > 350$ GeV and at least one electron or muon with $p_T > 15$ GeV, where these variables are computed with online (trigger-level) quantities and typically have somewhat poorer resolution than the corresponding offline variables. To ensure high trigger efficiency with respect to the offline definition of lepton isolation described in the previous section (mini-isolation), we designed these triggers with very loose lepton isolation requirements and fixed the isolation cone size to $R = 0.2$. For events passing the offline selection, the total trigger efficiencies, measured in data control samples that are independently triggered, are found to be $(95.1 \pm 1.1)\%$ for the muon

Table 1: Event yields obtained from simulated event samples, as the event selection criteria are applied. The category *Other* includes Drell–Yan, $\mathrm{t\bar{t}H}(\rightarrow \mathrm{b\bar{b}})$, $\mathrm{t\bar{t}t\bar{t}}$, WZ, and WW. The yields for $\mathrm{t\bar{t}}$ events in fully hadronic final states are included in the QCD multijet category. The category $\mathrm{t\bar{t}V}$ includes $\mathrm{t\bar{t}W}$, $\mathrm{t\bar{t}Z}$, and $\mathrm{t\bar{t}}\gamma$. The benchmark signal models, T1tttt(NC) and T1tttt(C), are described in Section 3. The event selection requirements listed above the horizontal line in the middle of the table are defined as the *baseline selection*. The background estimates before the H_T requirement are not specified because some of the simulated event samples do not extend to the low H_T region. Given the size of the MC samples described in Section 3, rows with zero yield have statistical uncertainties of at most 0.16 events, and below 0.05 events in most cases.

$\mathcal{L} = 2.3\,\mathrm{fb}^{-1}$	Other	QCD	$\mathrm{t\bar{t}V}$	Single t	W+jets	$\mathrm{t\bar{t}}$ (1ℓ)	$\mathrm{t\bar{t}}$ (2ℓ)	SM bkg.	T1tttt(NC)	T1tttt(C)
No selection	—	—	—	—	—	—	—	—	31.3	190.0
1ℓ, $p_\mathrm{T} > 20\,\mathrm{GeV}$	—	—	—	—	—	—	—	—	11.9	68.7
$H_\mathrm{T} > 500\,\mathrm{GeV}$	4131.9	31831.5	721.9	2926.6	31885.1	27628.7	3357.8	102483.4	11.9	44.9
$E_\mathrm{T}^\mathrm{miss} > 200\,\mathrm{GeV}$	310.6	154.7	89.1	457.2	4343.1	2183.6	584.0	8122.3	10.5	21.5
$N_\mathrm{jets} \geq 6$, $p_\mathrm{T} > 30\,\mathrm{GeV}$	27.3	8.0	36.8	82.8	278.7	792.3	171.4	1397.4	9.6	20.4
$N_\mathrm{b} \geq 1$	9.4	2.7	29.6	63.9	66.3	632.2	137.4	941.4	9.1	19.1
$M_J > 250\,\mathrm{GeV}$	6.7	2.6	22.6	43.8	46.1	455.2	87.2	664.2	9.0	16.5
$m_\mathrm{T} > 140\,\mathrm{GeV}$	0.7	1.4	3.0	3.5	1.2	5.5	32.5	47.9	7.0	9.2
$M_J > 400\,\mathrm{GeV}$	0.4	0.8	1.1	1.4	0.6	2.8	9.7	16.7	6.4	4.5
$N_\mathrm{b} \geq 2$	0.16	0.04	0.55	0.68	0.00	1.29	4.52	7.24	4.87	3.47
$E_\mathrm{T}^\mathrm{miss} > 400\,\mathrm{GeV}$	0.02	0.00	0.12	0.31	0.00	0.07	0.72	1.24	3.60	1.48
$N_\mathrm{jets} \geq 9$, $p_\mathrm{T} > 30\,\mathrm{GeV}$	0.01	0.00	0.03	0.00	0.00	0.01	0.11	0.16	1.64	1.00

channel and $(94.1 \pm 1.2)\%$ for the electron channel and are independent of the analysis variables within the uncertainties. These efficiencies are applied to the simulation as a correction.

The offline event selection is summarized in Table 1, which lists the event yields expected from simulation for both SM background processes and for the two benchmark T1tttt signal models. We select events with exactly one isolated charged lepton (an electron or a muon), $H_\mathrm{T} > 500\,\mathrm{GeV}$, $E_\mathrm{T}^\mathrm{miss} > 200\,\mathrm{GeV}$, and at least six jets, at least one of which is b-tagged. After this set of requirements, referred in the following as the *baseline selection*, more than 80% of the remaining SM background arises from $\mathrm{t\bar{t}}$ production. The contributions from events with a single top quark or a W boson in association with jets are each about 6–7%. The background from QCD multijet events after the baseline selection is negligible due to the combination of leptonic, $E_\mathrm{T}^\mathrm{miss}$, and N_jets requirements.

After the baseline selection requirements are applied, events are binned in several other kinematic variables, both to increase the signal sensitivity and to define control regions, as described in Section 6.1. To illustrate the effect of additional requirements, Table 1 lists the expected yields for examples of event selection requirements on M_J, m_T, N_jets, and N_b. The events satisfying the baseline selection are divided in the M_J-m_T plane into a signal region, defined by the additional requirements $M_J > 400\,\mathrm{GeV}$ and $m_\mathrm{T} > 140\,\mathrm{GeV}$, and three control samples, bounded by $M_J > 250\,\mathrm{GeV}$, that are used in the background estimation. Approximately 37% of signal T1tttt events are selected with the single-lepton requirement only. In non-compressed spectrum models, for which $m_{\tilde{\mathrm{g}}}$ is significantly larger than $m_{\tilde{\chi}_1^0}$, more than half of the events passing the lepton requirement lie in the signal region. For compressed spectrum models, where $m_{\tilde{\chi}_1^0} \approx m_{\tilde{\mathrm{g}}} - 2m_\mathrm{t}$, the M_J, H_T, and $E_\mathrm{T}^\mathrm{miss}$ spectra become much softer and, as a result, only 5–10% of the single-lepton signal events are selected.

As shown in Fig. 3, backgrounds with a single W boson decaying leptonically are strongly suppressed after the $m_\mathrm{T} > 140\,\mathrm{GeV}$ requirement, so the total SM background in the signal region is dominated by dilepton $\mathrm{t\bar{t}}$ events. This dilepton background falls into two categories, which make roughly equal contributions. The first involves an identified electron or muon

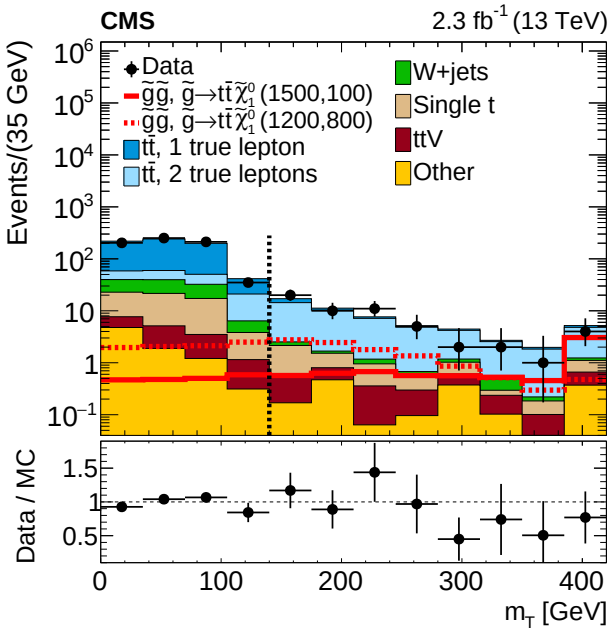

Figure 3: Distribution of m_{T} in data and simulated event samples after the baseline selection is applied. The background contributions shown here are from simulation, and their total yield is normalized to the number of events observed in data. The signal distributions are normalized to the expected cross sections. The dashed vertical line indicates the $m_{\mathrm{T}} > 140\,\mathrm{GeV}$ threshold that separates the signal regions from the control samples.

and a hadronically decaying τ from W decay. The second source involves two leptons, each of which is an electron or a muon. One of the leptons fails to satisfy the lepton selection criteria, which include the p_{T} and isolation requirements. This missed lepton can be produced either directly or indirectly in W decay, where in the indirect case the lepton is the daughter of a τ.

6 Background estimation

6.1 Method

The prediction of the background yields in each of the signal bins takes advantage of the fact that the M_J and m_{T} distributions of events with a significant amount of ISR are largely uncorrelated. The correlation coefficients for the single-lepton and dilepton $\mathrm{t\bar{t}}$ events in the M_J-m_{T} plane after the baseline selection (as shown in Fig. 4) are small, in the range 0.03 to 0.05. The absence of a substantial correlation allows us to measure the M_J distribution of the background at low m_{T} with good statistical precision, and extrapolate it to high m_{T}. The underlying explanation for this behavior is not immediately obvious, given that low-m_{T} events originate mainly from $\mathrm{t\bar{t}}$ events where only one of the top quarks decays leptonically (1ℓ $\mathrm{t\bar{t}}$), while the high-m_{T} regions are dominated by dilepton $\mathrm{t\bar{t}}$ events (2ℓ $\mathrm{t\bar{t}}$). In particular, as shown in Fig. 2 (left), in the absence of significant ISR, the dileptonic $\mathrm{t\bar{t}}$ events have a softer M_J spectrum than single-lepton $\mathrm{t\bar{t}}$ events, simply because the reconstructed mass of a leptonically decaying top quark does not include the undetected neutrino.

In events with substantial ISR, however, the contributions to M_J from the accidental overlap of jets can dominate the contributions due to the intrinsic mass of the top quarks. This effect is illustrated in Fig. 5, which compares the N_{jets} and M_J distributions of single-lepton and dilepton $\mathrm{t\bar{t}}$ events at high and low m_{T} after the baseline selection is applied. Since we require at least

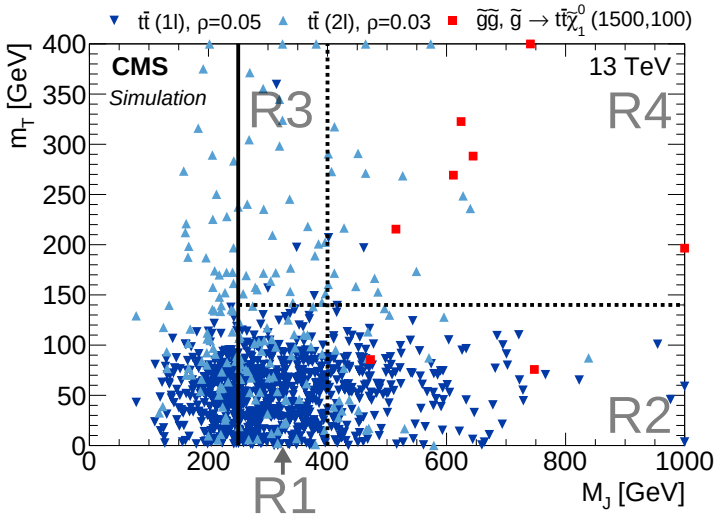

Figure 4: Distribution of simulated single-lepton $\mathrm{t\bar{t}}$ events (dark-blue triangles), dilepton $\mathrm{t\bar{t}}$ events (light-blue inverted triangles), and T1tttt(1500,100) events (red squares) in the M_J-m_T plane after the baseline selection. Each marker represents one expected event at 2.3 fb^{-1}. Overflow events are placed on the edge of the plot. The values of the correlation coefficients ρ for each background process are given in the legend. Region R4 is the nominal signal region, while R1, R2, and R3 serve as control regions. The small signal contributions in the control regions are taken into account in one of the global fits, as discussed in the text.

6 jets, single-lepton $\mathrm{t\bar{t}}$ events must have at least 2 ISR jets and dilepton $\mathrm{t\bar{t}}$ events must have at least 4. In this regime, the probability of additional ISR jets is similar for events with a given number of partons of similar momenta, and, as a result, the number of objects contributing to M_J (jets plus the reconstructed lepton) is comparable in 1ℓ and 2ℓ $\mathrm{t\bar{t}}$ events. When these ISR jets overlap with the top quark decay products, the masses of the resulting large-R jets are dominated by the accidental overlap and, thus, the shapes of the M_J distribution of 1ℓ and 2ℓ $\mathrm{t\bar{t}}$ events become more similar. This is the case for $M_J > 250$ GeV, where Fig. 5 (right) shows that the distributions of the 1ℓ and 2ℓ $\mathrm{t\bar{t}}$ backgrounds have nearly the same shape, and the low-m_T to high-m_T extrapolation is warranted.

We thus divide the M_J-m_T plane into four regions, three control regions (CR) and one signal region (SR):

- Region R1 (CR): $m_\mathrm{T} \leq 140\,\mathrm{GeV},\ 250 \leq M_J \leq 400\,\mathrm{GeV}$
- Region R2 (CR): $m_\mathrm{T} \leq 140\,\mathrm{GeV},\ M_J > 400\,\mathrm{GeV}$
- Region R3 (CR): $m_\mathrm{T} > 140\,\mathrm{GeV},\ 250 \leq M_J \leq 400\,\mathrm{GeV}$
- Region R4 (SR): $m_\mathrm{T} > 140\,\mathrm{GeV},\ M_J > 400\,\mathrm{GeV}$.

These regions are further subdivided into 10 bins of $E_\mathrm{T}^\mathrm{miss}$, N_jets, and N_b to increase signal sensitivity:

- Six bins with $200 < E_\mathrm{T}^\mathrm{miss} \leq 400\,\mathrm{GeV}$: $(6 \leq N_\mathrm{jets} \leq 8, N_\mathrm{jets} \geq 9) \times (N_\mathrm{b} = 1, N_\mathrm{b} = 2, N_\mathrm{b} \geq 3)$
- Four bins with $E_\mathrm{T}^\mathrm{miss} > 400\,\mathrm{GeV}$: $(6 \leq N_\mathrm{jets} \leq 8, N_\mathrm{jets} \geq 9) \times (N_\mathrm{b} = 1, N_\mathrm{b} \geq 2)$,

where the multiplication indicates that the binning is two dimensional in N_jets and N_b. Given that the main background processes have two or fewer b quarks, the total SM contribution to the $N_\mathrm{b} \geq 3$ bins is very small and is driven by the b-tag fake rate. Signal events in the T1tttt and

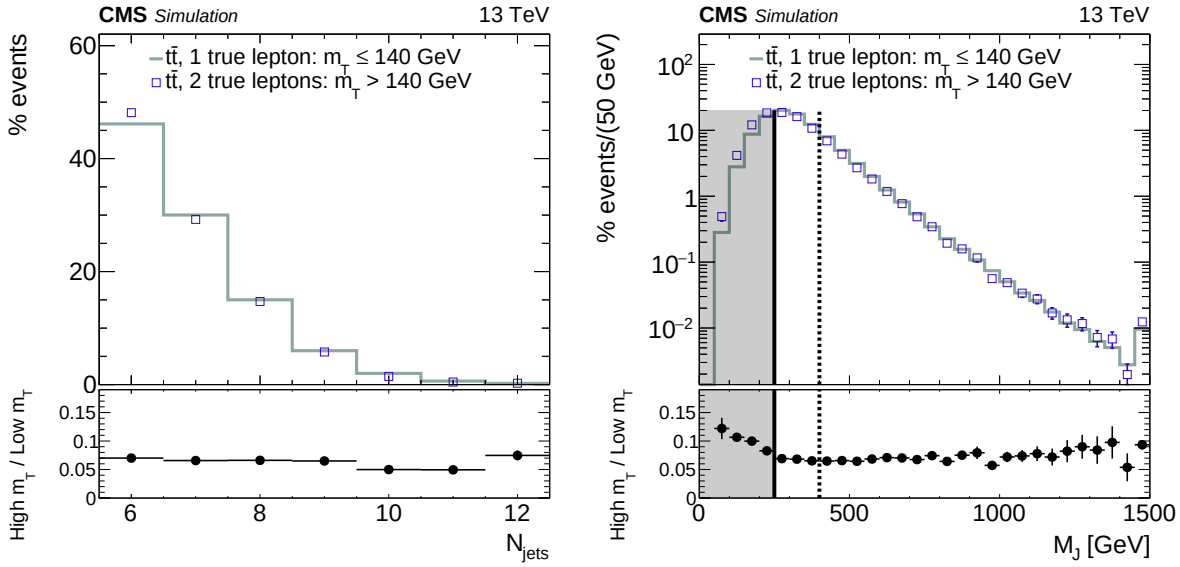

Figure 5: Comparison of N_{jets} and M_J distributions, normalized to the same area, in simulated $\mathrm{t\bar{t}}$ events with two true leptons at high m_{T} and one true lepton at low m_{T}, after the baseline selection is applied. The shapes of these distributions are similar. These two contributions are the dominant backgrounds in their respective m_{T} regions. The dashed vertical line on the right-hand plot indicates the $M_J > 400\,\text{GeV}$ threshold that separates the signal regions from the control samples. The shaded region corresponding to $M_J < 250\,\text{GeV}$ is not used in the background estimation.

T5tttt models are expected to populate primarily the bins with $N_{\text{b}} \geq 2$, while bins with $N_{\text{b}} = 1$ mainly serve to test the method in a background dominated region.

To obtain an estimate of the background rate in each of the signal bins, a modified version of an "ABCD" method is used. Here, the symbols A, B, C, and D refer to four regions in a two-dimensional space in the data, where one of the regions is dominated by signal and the other three by backgrounds. In a standard ABCD method, the background rate in the signal region is estimated from the yields in three control regions with the expression

$$\mu_{\text{R4}}^{\text{bkg}} = N_{\text{R2}}\, N_{\text{R3}} / N_{\text{R1}}, \tag{4}$$

where the labels on the regions correspond to those shown in Fig. 4. The background prediction is unbiased in the limit that the two variables that define the plane (in this case, M_J and m_{T}) are uncorrelated. The effect of any residual correlation is corrected with factors κ that can be obtained from simulated event samples:

$$\kappa = \frac{N_{\text{R4}}^{\text{MC,bkg}} / N_{\text{R3}}^{\text{MC,bkg}}}{N_{\text{R2}}^{\text{MC,bkg}} / N_{\text{R1}}^{\text{MC,bkg}}}. \tag{5}$$

When the two ABCD variables are uncorrelated or nearly so, the κ factors are close to unity. This procedure ignores potential signal contamination in the control regions, which is accounted for by incorporating the constraints in Eqs. 4 and 5 into a fit that includes both signal and background components, as described in Section 6.2.

In principle, the background in the 10 signal bins could be estimated by applying this procedure in 10 independent planes. However, this procedure would incur large statistical uncertainties in some bins due to low numbers of events in R3. This problem is especially important in bins

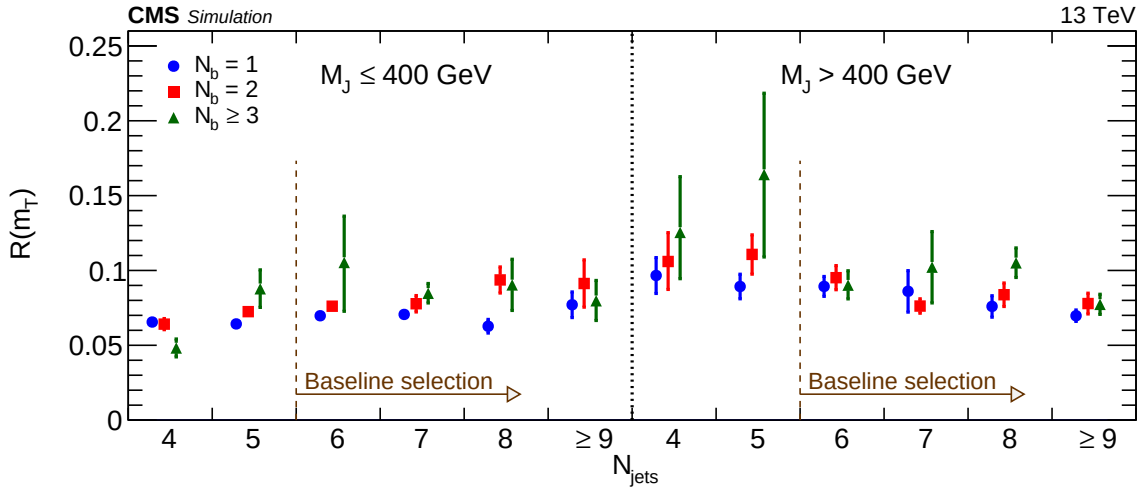

Figure 6: The ratio $R(m_T)$ of high-m_T (R3 and R4) to low-m_T (R1 and R2) event yields for the simulated SM background, as a function of N_{jets} and N_b. The baseline selection requires $N_{jets} \geq 6$. The uncertainties shown are statistical only.

with a high number of jets, where the M_J spectrum shifts to higher values and the number of background events expected in R4 can exceed the background in R3.

To alleviate this problem, we exploit the fact that, after the baseline selection, the background is dominated by just one source ($t\bar{t}$ events), and the shapes of the N_{jets} distributions are nearly identical for the single-lepton and dilepton components (due to the large amounts of ISR). As a result, the m_T distribution is approximately independent of N_{jets} and N_b. We study this behavior with the ratio of the number of events at high to low m_T:

$$R(m_T) \equiv \frac{N(m_T > 140\,\text{GeV})}{N(m_T \leq 140\,\text{GeV})}. \tag{6}$$

Because, as seen in Fig. 6, the values of $R(m_T)$ do not vary substantially across N_{jets} and N_b bins, the predicted value of $R(m_T)$ is not sensitive to the modeling of the distributions of those quantities. We exploit this result by integrating the yields of the low-M_J regions (R1 and R3) over the N_{jets} and N_b bins for each E_T^{miss} bin. This procedure increases the statistical power of the ABCD method but also introduces a correlation among the predictions (Eq. 4) for the N_{jets} and N_b bins associated with a given E_T^{miss} bin. Figure 7 shows the κ factors for the 10 signal bins after summing over N_{jets} and N_b in R1 and R3. In all cases, their values are close to unity.

6.2 Implementation

The method outlined in Section 6.1 is implemented with a likelihood function that incorporates the statistical and systematic uncertainties in κ, accounts for correlations arising from the common R1 and R3 yields, and corrects for signal contamination in the control regions.

The SM background contribution for each region is described as follows. We define μ_{Ri}^{bkg} as the estimated (Poisson) mean background in each region Ri, with $i = 1,2,3,4$. Then, in an ABCD background calculation, these four rates can be expressed in terms of three floating fit parameters μ, $R(m_T)$, and $R(M_J)$, and the correlation correction factor κ, as

$$\begin{aligned} \mu_{R1}^{bkg} &= \mu, & \mu_{R2}^{bkg} &= \mu\, R(M_J), \\ \mu_{R3}^{bkg} &= \mu\, R(m_T), & \mu_{R4}^{bkg} &= \kappa\, \mu\, R(M_J)\, R(m_T). \end{aligned} \tag{7}$$

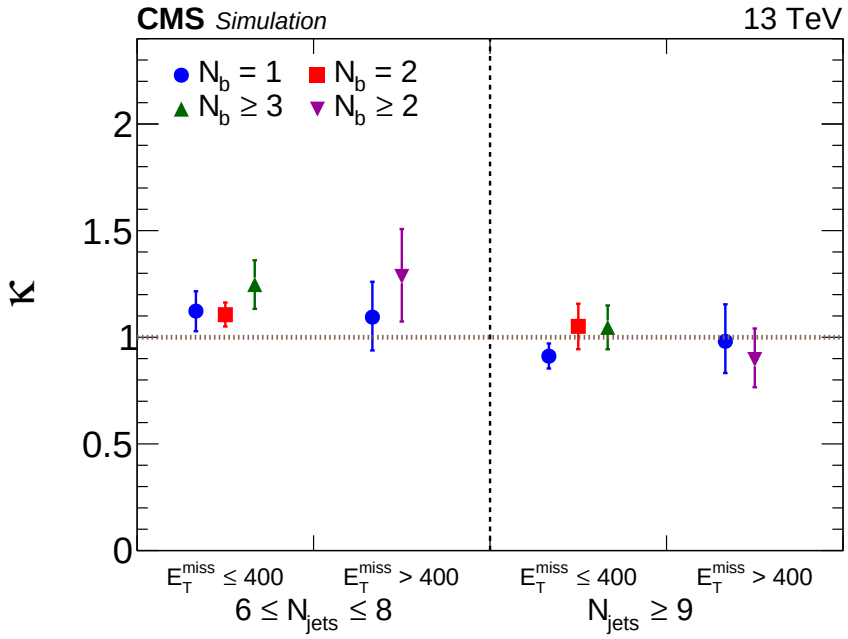

Figure 7: Values of the double-ratio κ in each of the 10 signal bins, calculated using the simulated SM background. The κ factors are close to unity, indicating the small correlation between M_J and m_{T}. The uncertainties shown are statistical only.

Here, μ is the background rate fit parameter for R1, $R(M_J)$ is the ratio of the R2 to R1 rates, and $R(m_{\mathrm{T}})$ is the ratio of the R3 to R1 rates. The quantity κ is given by Eq. 5 after replacing the yields $N_{\mathrm{R}i}^{\mathrm{MC,bkg}}$ by the background rate fit parameters $\mu_{\mathrm{R}i}^{\mathrm{MC,bkg}}$.

Similarly, we define $N_{\mathrm{R}i}^{\mathrm{data}}$ as the observed data yield in each region, $\mu_{\mathrm{R}i}^{\mathrm{MC,sig}}$ as the expected signal rate in each region, and r as the parameter quantifying the signal strength relative to the expected yield across all analysis regions. We can then write the likelihood function as

$$\mathcal{L} = \mathcal{L}_{\mathrm{ABCD}}^{\mathrm{data}}\,\mathcal{L}_{\kappa}^{\mathrm{MC}}\,\mathcal{L}_{\mathrm{sig}}^{\mathrm{MC}}, \tag{8}$$

$$\mathcal{L}_{\mathrm{ABCD}}^{\mathrm{data}} = \prod_{i=1}^{4}\prod_{k=1}^{N_{\mathrm{bins}}(\mathrm{R}i)} \mathrm{Poisson}(N_{\mathrm{R}i,k}^{\mathrm{data}} | \mu_{\mathrm{R}i,k}^{\mathrm{bkg}} + r\,\mu_{\mathrm{R}i,k}^{\mathrm{MC,sig}}), \tag{9}$$

$$\mathcal{L}_{\kappa}^{\mathrm{MC}} = \prod_{i=1}^{4}\prod_{k=1}^{N_{\mathrm{bins}}(\mathrm{R}i)} \mathrm{Poisson}(N_{\mathrm{R}i,k}^{\mathrm{MC,bkg}} | \mu_{\mathrm{R}i,k}^{\mathrm{MC,bkg}}), \tag{10}$$

$$\mathcal{L}_{\mathrm{sig}}^{\mathrm{MC}} = \prod_{i=1}^{4}\prod_{k=1}^{N_{\mathrm{bins}}(\mathrm{R}i)} \mathrm{Poisson}(N_{\mathrm{R}i,k}^{\mathrm{MC,sig}} | \mu_{\mathrm{R}i,k}^{\mathrm{MC,sig}}). \tag{11}$$

The indices k run over each of the $E_{\mathrm{T}}^{\mathrm{miss}}$, N_{jets}, and N_{b} bins defined in the previous section; these indices were suppressed in Eq. 7 for simplicity. Given the integration over N_{jets} and N_{b} at low M_J, $N_{\mathrm{bins}}(\mathrm{R1}) = N_{\mathrm{bins}}(\mathrm{R3}) = 2$, while $N_{\mathrm{bins}}(\mathrm{R2}) = N_{\mathrm{bins}}(\mathrm{R4}) = 10$.

In Eq. 8, $\mathcal{L}_{\mathrm{ABCD}}^{\mathrm{data}}$ accounts for the statistical uncertainty in the observed data yield in the four ABCD regions, and $\mathcal{L}_{\kappa}^{\mathrm{MC}}$ and $\mathcal{L}_{\mathrm{sig}}^{\mathrm{MC}}$ account for the uncertainty in the computation of the κ correction factor and signal shape, respectively, due to the finite size of the MC samples.

The systematic uncertainties in κ and the signal efficiency are described in the following sections. These effects are incorporated in the likelihood function as log-normal constraints with a

nuisance parameter for each uncorrelated source of uncertainty. These terms are not explicitly shown in the likelihood function above for simplicity.

The likelihood function defined in Eqs. 8–11 is employed in two separate types of fits that provide complementary but compatible background estimates based on an ABCD model. The first type of fit, which we call the *predictive fit*, allows us to more easily establish the agreement of the background predictions and the observations in the null (i.e., the background-only) hypothesis. We do this by excluding the observations in the signal regions in the likelihood (that is, by truncating the first product in Eq. 9 at $i = 3$) and fixing the signal strength r to 0. This procedure leaves as many unknowns as constraints: three *data* floating parameters (μ, $R(M_J)$, and $R(m_T)$) and three observations ($N^{\text{data}}_{\text{R}i,k}$ with $i = 1,2,3$) for each ABCD plane. In the likelihood function there are additional floating parameters associated with MC quantities, which have small uncertainties. As a result, the estimated background rates in regions R1, R2, and R3 converge to the observed values in those bins, and we obtain predictions for the signal regions that do not depend on the observed $N^{\text{data}}_{\text{R4}}$. The predictive fit thus converges to the standard ABCD method, and the likelihood machinery becomes just a convenient way to solve the system of equations and propagate the various uncertainties.

Additionally, we implement a *global fit* which, by making use of the observations in the signal regions, can provide an estimate of the signal strength r, while allowing for signal events to populate the control regions. This is achieved by including all four observations, $N^{\text{data}}_{\text{R}i,k}$ with $i = 1,2,3,4$, in the likelihood function. Since there are four observations and three floating background parameters in each ABCD plane, there are enough constraints for the signal strength also to be determined in the fit.

6.3 Systematic uncertainties

This section describes the systematic uncertainties in the background prediction, which are incorporated into the analysis as an uncertainty in the κ correction. Because the dominant background arises from 2ℓ $\mathrm{t\bar{t}}$ events, we use a control sample with two reconstructed leptons to validate our background estimation procedure and to quantify the associated uncertainty. The resulting uncertainty is augmented with simulation-based studies of effects that are not covered by this dilepton test. Table 2 summarizes all of the uncertainties in the background prediction.

The ability of the ABCD method to predict the 2ℓ $\mathrm{t\bar{t}}$ background is studied using a modified ABCD plane, in which the high-m_T regions, R3 and R4, are replaced with regions D3 and D4, which have two reconstructed leptons. These regions have low and high M_J, respectively, just as R3 and R4. The events in D3 and D4 pass the same selection as those in R3 and R4, except for the following changes: N_{jets} bin boundaries are lowered by one to keep the number of large-R jet constituents the same as in the single-lepton samples; the m_T requirement is not applied; and events with $N_b = 0$ are included to increase the size of the event sample, while events with $N_b \geq 3$ are excluded to avoid signal contamination. We perform this test only for low E_T^{miss} to further avoid the potentially large signal contribution in the high-E_T^{miss} region. The low-M_J regions (R1 and D3) are integrated over N_{jets}, while the high-M_J regions (R2 and D4) are binned in low and high N_{jets}. The predictive fit is then used to predict the D4 event yields for both N_{jets} bins. We predict 11.0 ± 2.3 (1.5 ± 0.5) events for the low (high) N_{jets} bin, and we observe 12 (2) events. Given the good agreement between prediction and observation, the statistical precision of the test is taken as a systematic uncertainty in κ. These uncertainties are 37% and 88% for the low- and high-N_{jets} regions, respectively.

Since the event composition of regions D3 and D4 is not fully representative of that in R3

Table 2: Summary of uncertainties in the background predictions. All entries in the table except for data sample size correspond to a relative uncertainty on κ. The ranges indicate the spread of each uncertainty across the signal bins. Uncertainties from a particular source are treated as fully correlated across bins, while uncertainties from different sources are treated as uncorrelated.

Source	Fractional uncertainty [%]
Data sample size	28–118
Dilepton control sample test	37–88
Simulation sample size	5–17
Jet energy resolution	2–10
Jet energy corrections	1–5
ISR p_{T}	1–5
Top p_{T}	1–4
Non-$\mathrm{t\bar{t}}$ background	2–11

and R4, we perform studies on potential additional sources of systematic uncertainty in the simulation. We find that the main source of 1ℓ $\mathrm{t\bar{t}}$ events in the high-m_{T} region is jet energy mismeasurement. We study the impact of mismodeling the size of this contribution by smearing the jet energies by an additional 50% with respect to the jet energy resolution measured in data [70] and calculating the corresponding shift in κ. To ensure that there are no further significant differences between the M_J shapes of events reconstructed with one or two leptons, we also calculate the shift in κ due to jet energy corrections, potential ISR p_{T} and top quark p_{T} mismodeling, as well as the amount of non-$\mathrm{t\bar{t}}$ background. Even though each of these can alone have a significant effect on the M_J shape, the κ factor, as a double ratio, remains largely unaffected (Table 2). Including these uncertainties in the likelihood fit produces a negligible contribution to the total uncertainty.

7 Results and interpretation

Figure 8 shows the two-dimensional distribution of the data in the m_{T}-M_J plane after the baseline selection, but with the additional requirement $N_{\mathrm{b}} \geq 2$. The baseline requirements include $E_{\mathrm{T}}^{\mathrm{miss}} > 200\,\mathrm{GeV}$ and $N_{\mathrm{jets}} \geq 6$, but no further event selection is applied. For comparison, the plot also shows the expected total SM background based on simulation, as well as a particular sample of the expected signal distribution. The overall distribution of events in data is consistent with the background expectation, where the majority of events are concentrated at low m_{T} and M_J. In R4, the nominal signal region, we observe only two events in data, while, as shown in Table 3, the predicted SM background is about 5 events. The T1tttt(1500,100) (NC) model would be expected to contribute 5 additional events to R4.

The validity of the central assumption of the background estimation method can be checked in the nearly signal-free $N_{\mathrm{b}} = 1$ region by comparing the M_J shapes observed in the high- and low-m_{T} regions in data. Figure 9 (left) shows the M_J shapes in the $N_{\mathrm{b}} = 1$ sample, integrating over the N_{jets} and $E_{\mathrm{T}}^{\mathrm{miss}}$ bins. The low m_{T} data have been normalized to the overall yields in the corresponding high-m_{T} data. The shapes of the M_J distributions for the high- and low-m_{T} regions are consistent. Figure 9 (right) shows that the corresponding distributions in the $N_{\mathrm{b}} \geq 2$ sample are also consistent, as expected in the absence of signal.

Table 3 summarizes the observed event yields, the fitted backgrounds, and the expected signal yields for the two T1tttt benchmark model points. Two background estimates are given: the

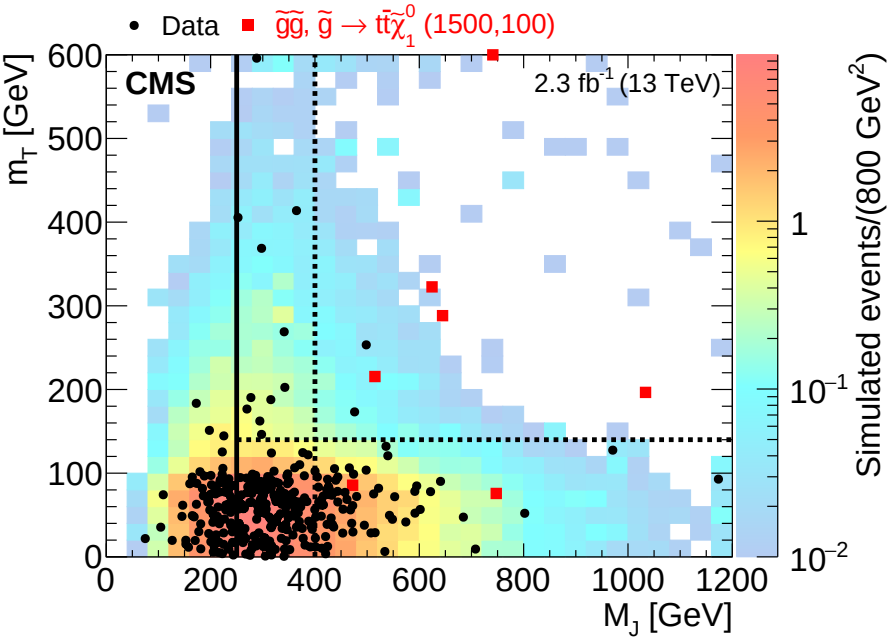

Figure 8: Two-dimensional distributions for data and simulated event samples in the variables m_T and M_J in the $N_b \geq 2$ region after the baseline selection. The distributions integrate over the N_{jets} and E_T^{miss} bins. The black dots are the data; the colored histogram is the total simulated background, normalized to the data; and the red dots are a particular signal sample drawn from the expected distribution for gluino pair production in the T1tttt model with $m_{\tilde{g}} = 1500\,\text{GeV}$ and $m_{\tilde{\chi}_1^0} = 100\,\text{GeV}$ for $2.3\,\text{fb}^{-1}$. Overflow events are shown on the edges of the plot. The definitions of the signal and control regions are the same as those shown in Fig. 4.

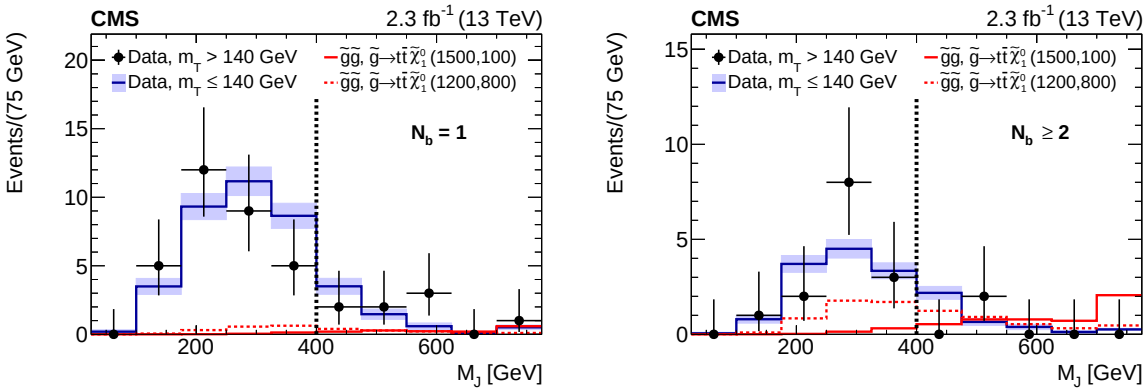

Figure 9: Comparison of the M_J distributions for low- and high-m_T in data with $N_b = 1$ (left) and $N_b \geq 2$ (right) after the baseline selection. The expected M_J distributions of the two benchmark T1tttt scenarios for $m_T > 140$ GeV are overlaid. The distributions integrate over the N_{jets} and E_T^{miss} bins. The low-m_T distribution is normalized to the number of events in the high-m_T region. The dashed vertical lines indicate the $M_J > 400\,\text{GeV}$ threshold that separates the signal regions from the control samples.

predictive fit (PF), which uses only the yields in regions R1, R2, and R3, and the global fit (GF), which also incorporates region R4, as described in Section 6. In both versions of the fit, the signal strength r is fixed to zero, giving results that are model independent. (When setting limits on individual models, we allow r to float, as discussed below.) The rows labeled R4 give the results for each of the ten signal regions, as well as the corresponding κ factors.

In the absence of signal, the predictive fit and the version of the global fit performed under the null hypothesis, $r = 0$, should be consistent with each other. However, because the global fit incorporates more information, specifically the yields in R4, this fit has a smaller uncertainty. The regions with $N_b = 1$ have small expected contributions from signal. Summing over all four such signal regions (R4), the number of estimated background events from the PF and GF are 6.1 ± 2.2 and 5.5 ± 1.3, respectively, compared with 8 events observed in data. The consistency between the two predictions and between the predicted and observed yields in the R4 regions with $N_b = 1$, where the signal contribution is expected to be small, serves as a further check on the background estimation method. Summing the yields over the six signal bins with $N_b \geq 2$, the number of estimated background events from PF and GF is 5.6 ± 1.6 and 4.9 ± 1.0, respectively. In data, we observe 2 events, lower than, but consistent with the background-only hypothesis.

Given the absence of any significant excess, the results are interpreted first as exclusion limits on the production cross section for T1tttt model points as a function of $m_{\tilde{g}}$ and $m_{\tilde{\chi}_1^0}$. Table 4 shows the ranges for the systematic uncertainties associated with predictions for the expected signal yields, including those on the signal efficiency. The largest uncertainties arise from the jet energy corrections and from the modeling of ISR. These uncertainties are generally in the range 10–20% but can increase to $\sim$30% as the mass splitting between the gluino and LSP decreases [77]. The uncertainty associated with the renormalization and factorization scales is determined by varying the scales independently up and down by a factor of two; these are applied only as an uncertainty in the signal shape, i.e., the cross section is held constant. The uncertainty associated with the b tagging efficiency is in the range 1–15%. Uncertainties due to pileup, luminosity [78], lepton selection, and trigger efficiency are found to be $\leq$ 5%. Uncertainties for each particular source are treated as fully correlated across bins.

A 95% confidence level (CL) upper limit on the production cross section is estimated using the modified frequentist CL_S method [79–81], with a one-sided profile likelihood ratio test statistic. For this test, we perform the global fit under the background-only and background-plus-signal (r floating) hypotheses. The statistical uncertainties from data counts in the control regions are modeled by the Poisson terms in Eq. 9. All systematic uncertainties are multiplicative and are treated as log-normal distributions. Exclusion limits are also estimated for $\pm 1\sigma$ variations on the production cross section based on the NLO+NLL calculation [39].

Figure 10 shows the corresponding excluded region at a 95% CL for the T1tttt model in the $m_{\tilde{g}} - m_{\tilde{\chi}_1^0}$ plane. At low $\tilde{\chi}_1^0$ mass we exclude gluinos with masses of up to 1600 GeV. The highest limit on the $\tilde{\chi}_1^0$ mass is 800 GeV, attained for $m_{\tilde{g}}$ of approximately 1300 GeV. The observed limits are within the 1σ uncertainty in the expected limits. The central value is slightly higher because the observed event yield is less than the SM background prediction, as shown in Table 3.

In the context of natural SUSY models, it is important to extend the interpretation to scenarios in which the top squark is lighter than the gluino. Rather than considering a large set of models with independently varying top squark masses, we consider the extreme case in which the top squark has approximately the smallest mass consistent with two-body decay, $m_{\tilde{t}_1} \approx m_t + m_{\tilde{\chi}_1^0}$, for a range of gluino and neutralino masses. The decay kinematics for such extreme, com-

Table 3: Observed and predicted event yields for the signal regions (R4) and background regions (R1–R3) in data (2.3 fb^{-1}). Expected yields for the two SUSY T1tttt benchmark scenarios are also given. The results from two types of fits are reported: the predictive fit (PF) and the version of the global fit (GF) performed under the assumption of the null hypothesis ($r = 0$). The predictive fit uses the observed yields in regions R1, R2, and R3 only and is effectively just a propagation of uncertainties. The global fit uses all four regions. The values of κ obtained from the simulation fit are also listed. The first uncertainty in κ is statistical, while the second corresponds to the total systematic uncertainty. The benchmark signal models, T1tttt(NC) and T1tttt(C), are described in Section 3.

Region: bin	κ	T1tttt(NC)	T1tttt(C)	Fitted μ^{bkg} (PF)	Fitted μ^{bkg} (GF)	Obs.
$200 < E_{\text{T}}^{\text{miss}} \leq 400\,\text{GeV}$						
R1: all N_{jets}, N_{b}	—	0.1	3.2	336.0 ± 18.3	335.3 ± 18.2	336
R2: $6 \leq N_{\text{jets}} \leq 8$, $N_{\text{b}} = 1$	—	0.1	0.2	47.1 ± 6.9	49.5 ± 6.9	47
R2: $N_{\text{jets}} \geq 9$, $N_{\text{b}} = 1$	—	0.1	0.3	7.0 ± 2.6	7.5 ± 2.7	7
R2: $6 \leq N_{\text{jets}} \leq 8$, $N_{\text{b}} = 2$	—	0.1	0.3	42.0 ± 6.5	41.1 ± 6.2	42
R2: $N_{\text{jets}} \geq 9$, $N_{\text{b}} = 2$	—	0.1	0.5	7.0 ± 2.6	6.6 ± 2.5	7
R2: $6 \leq N_{\text{jets}} \leq 8$, $N_{\text{b}} \geq 3$	—	0.1	0.2	12.0 ± 3.5	11.1 ± 3.2	12
R2: $N_{\text{jets}} \geq 9$, $N_{\text{b}} \geq 3$	—	0.2	0.6	1.0 ± 1.0	0.9 ± 0.9	1
R3: all N_{jets}, N_{b}	—	0.2	3.8	21.0 ± 4.6	21.6 ± 4.2	21
R4: $6 \leq N_{\text{jets}} \leq 8$, $N_{\text{b}} = 1$	$1.12 \pm 0.09 \pm 0.43$	0.2	0.2	3.3 ± 1.4	3.6 ± 1.0	6
R4: $N_{\text{jets}} \geq 9$, $N_{\text{b}} = 1$	$0.91 \pm 0.06 \pm 0.81$	0.2	0.4	0.4 ± 0.3	0.4 ± 0.2	1
R4: $6 \leq N_{\text{jets}} \leq 8$, $N_{\text{b}} = 2$	$1.11 \pm 0.06 \pm 0.42$	0.3	0.4	2.9 ± 1.2	2.9 ± 0.8	2
R4: $N_{\text{jets}} \geq 9$, $N_{\text{b}} = 2$	$1.05 \pm 0.11 \pm 0.94$	0.3	0.6	0.5 ± 0.3	0.4 ± 0.2	0
R4: $6 \leq N_{\text{jets}} \leq 8$, $N_{\text{b}} \geq 3$	$1.25 \pm 0.11 \pm 0.47$	0.3	0.3	0.9 ± 0.4	0.9 ± 0.3	0
R4: $N_{\text{jets}} \geq 9$, $N_{\text{b}} \geq 3$	$1.05 \pm 0.10 \pm 0.93$	0.3	0.7	0.1 ± 0.1	0.1 ± 0.1	0
$E_{\text{T}}^{\text{miss}} > 400\,\text{GeV}$						
R1: all N_{jets}, N_{b}	—	0.1	0.5	16.0 ± 4.0	17.1 ± 4.0	16
R2: $6 \leq N_{\text{jets}} \leq 8$, $N_{\text{b}} = 1$	—	0.2	0.1	8.0 ± 2.8	6.8 ± 2.5	8
R2: $N_{\text{jets}} \geq 9$, $N_{\text{b}} = 1$	—	0.1	0.2	1.0 ± 1.0	1.7 ± 1.2	1
R2: $6 \leq N_{\text{jets}} \leq 8$, $N_{\text{b}} \geq 2$	—	0.5	0.3	3.0 ± 1.7	2.5 ± 1.4	3
R2: $N_{\text{jets}} \geq 9$, $N_{\text{b}} \geq 2$	—	0.4	0.6	1.0 ± 1.0	0.9 ± 0.9	1
R3: all N_{jets}, N_{b}	—	0.4	0.9	4.0 ± 2.0	2.9 ± 1.4	4
R4: $6 \leq N_{\text{jets}} \leq 8$, $N_{\text{b}} = 1$	$1.09 \pm 0.16 \pm 0.42$	0.7	0.2	2.2 ± 1.7	1.2 ± 0.7	0
R4: $N_{\text{jets}} \geq 9$, $N_{\text{b}} = 1$	$0.98 \pm 0.16 \pm 0.87$	0.4	0.3	0.2 ± 0.3	0.3 ± 0.2	1
R4: $6 \leq N_{\text{jets}} \leq 8$, $N_{\text{b}} \geq 2$	$1.29 \pm 0.22 \pm 0.50$	1.9	0.5	1.0 ± 0.8	0.5 ± 0.4	0
R4: $N_{\text{jets}} \geq 9$, $N_{\text{b}} \geq 2$	$0.90 \pm 0.14 \pm 0.80$	1.6	1.0	0.2 ± 0.3	0.1 ± 0.1	0

Table 4: Typical values of the signal-related systematic uncertainties. Uncertainties due to a particular source are treated as fully correlated between bins, while uncertainties due to different sources are treated as uncorrelated.

Source	Fractional uncertainty [%]
Lepton efficiency	1–5
Trigger efficiency	1
b tagging efficiency	1–15
Jet energy corrections	1–30
Renormalization and factorization scales	1–5
Initial state radiation	1–35
Pileup	5
Integrated luminosity	3

pressed mass spectrum models correspond to the lowest signal efficiency for given values of $m_{\tilde{g}}$ and $m_{\tilde{\chi}_1^0}$, because the top quark and the $\tilde{\chi}_1^0$ are produced at rest in the top squark frame. As a consequence, the excluded signal cross section for fixed values of $m_{\tilde{g}}$ and $m_{\tilde{\chi}_1^0}$ and with $m_{\tilde{g}} > m_{\tilde{t}_1} \geq m_t + m_{\tilde{\chi}_1^0}$ is minimized around this extreme model point. For physical consistency, the signal model used in this study, both in the fit procedure and in the theoretical cross section used to obtain mass limits, includes not only gluino-pair production, but also direct $\tilde{t}_1\bar{\tilde{t}}_1$ production. However, the effect of the direct top squark contribution on the results is small, $\lesssim 2\%$ for $m_{\tilde{\chi}_1^0} > 400\,\text{GeV}$ and up to 20% for low values of $m_{\tilde{\chi}_1^0}$.

Figure 11 shows the excluded region in the $m_{\tilde{g}}$-$m_{\tilde{\chi}_1^0}$ plane for this combined model with both gluino-mediated top squark production and direct top squark pair production. The top squark mass is assumed to be 175 GeV above that of the neutralino. For most of the excluded region, the boundary is close to that obtained for the T1tttt model, showing that there is only a weak sensitivity to the value of the top squark mass. The uncertainty on the boundary of the excluded region for the T5tttt model is similar to that shown for the T1tttt model in Fig. 10. For $m_{\tilde{\chi}_1^0} > 150$ GeV, the excluded value of $m_{\tilde{g}}$ is typically within 60 GeV of that excluded for T1tttt. Models that have low values of $m_{\tilde{\chi}_1^0}$ show a reduced sensitivity because the neutralino carries very little momentum, reducing the value of m_T. In this kinematic region, the sensitivity to the signal is dominated by the events that have at least two leptonic W boson decays, which produce additional E_T^{miss}, as well as a tail in the m_T distribution. Although such dilepton events are nominally excluded in the analysis, a significant number of these signal events escape the dilepton veto. These events include both W decays to τ leptons that decay hadronically, and W decays to electrons or muons that are below kinematic thresholds or are outside of the detector acceptance.

8 Summary

Using a sample of proton-proton collisions at $\sqrt{s} = 13\,\text{TeV}$ with an integrated luminosity of $2.3\,\text{fb}^{-1}$, a search for supersymmetry is performed in the final state with a single lepton, b-tagged jets, and large missing transverse momentum. The search focuses on final states resulting from the pair production of gluinos, which subsequently decay via $\tilde{g} \to t\bar{t}\tilde{\chi}_1^0$, leading to high jet multiplicities.

A key feature of the analysis is the use of the variable M_J, the sum of the masses of large-R jets, which are formed by clustering anti-k_T $R = 0.4$ jets and leptons. Used in conjunction with

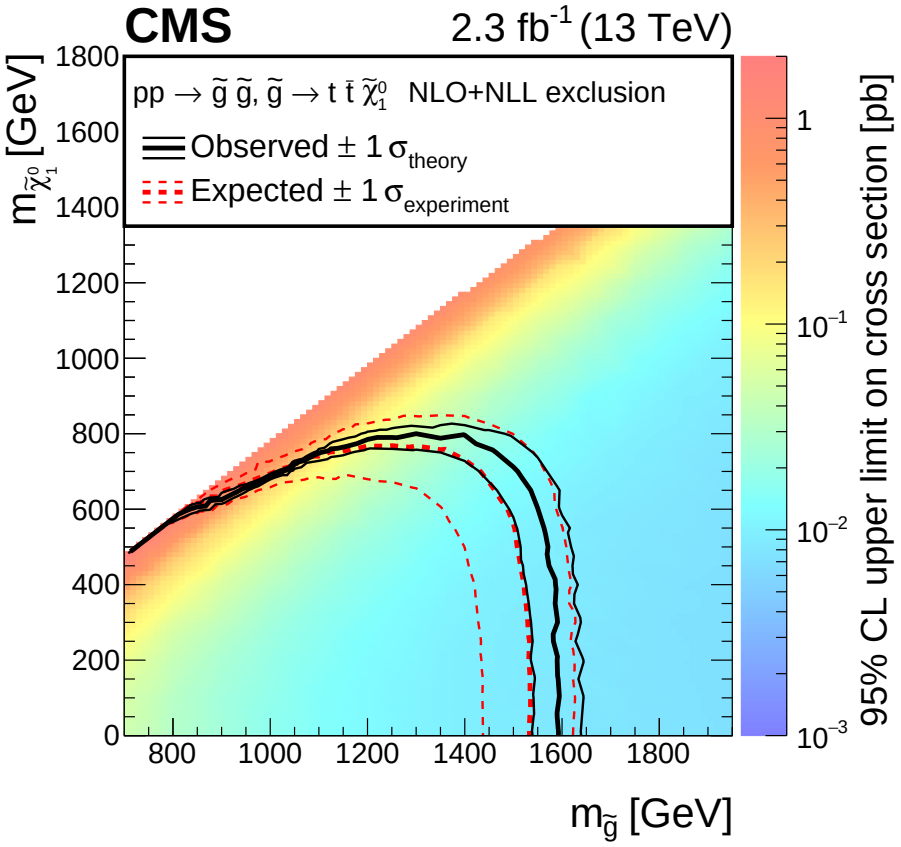

Figure 10: Interpretation of results in the T1tttt model. The colored regions show the upper limits (95% CL) on the production cross section for $pp \to \tilde{g}\tilde{g}, \tilde{g} \to t\bar{t}\tilde{\chi}_1^0$ in the $m_{\tilde{g}}$-$m_{\tilde{\chi}_1^0}$ plane. The curves show the expected and observed limits on the corresponding SUSY particle masses obtained by comparing the excluded cross section with theoretical cross sections.

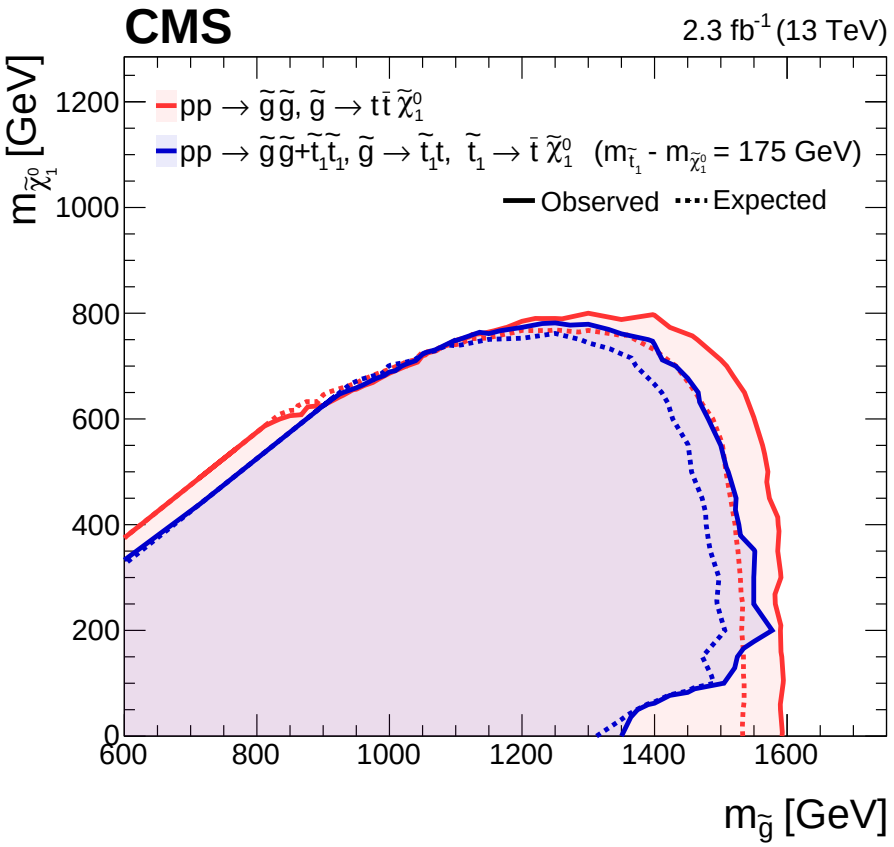

Figure 11: Excluded region (95% CL), shown in blue, in the $m_{\tilde{g}}$-$m_{\tilde{\chi}_1^0}$ plane for a model combining T5tttt, gluino pair production, followed by gluino decay to an on-shell top squark, together with a model for direct top squark pair production. The top squarks decay via the two-body process $\tilde{t} \to t\tilde{\chi}_1^0$. The neutralino and top squark masses are related by the constraint $m_{\tilde{t}_1} = m_{\tilde{\chi}_1^0} + 175\,\text{GeV}$. For comparison, the excluded region (95% CL) from Fig. 10 for the T1tttt model, which has three-body gluino decay, is shown in red. The small difference between the two boundary curves shows that the limits for the scenarios with two-body gluino decay have only a weak dependence on the top squark mass.

the variable m_{T}, the transverse mass of the system consisting of the lepton and the missing transverse momentum vector, M_J provides a powerful background estimation method that is well suited to this high jet multiplicity search.

After the baseline selection is applied, signal (R4) and control regions (R1, R2, and R3) are defined in the M_J-m_{T} plane, which are further divided into bins of $E_{\mathrm{T}}^{\mathrm{miss}}$, N_{jets}, and N_{b} to provide additional sensitivity. In regions R3 and R4, the requirement $m_{\mathrm{T}} > 140\,\mathrm{GeV}$ provides strong suppression of the single-lepton $\mathrm{t\bar{t}}$ background, so that dilepton $\mathrm{t\bar{t}}$ events dominate over all other background sources. For these dilepton events to enter a signal region, however, they must contain a substantial amount of initial-state radiation (ISR). For this extreme range of ISR jet momentum and multiplicity, the single-lepton and dilepton $\mathrm{t\bar{t}}$ events have very similar kinematic properties. The variables M_J and m_{T} are nearly uncorrelated, even though different processes dominate the low- and high-m_{T} regions. As a consequence, the low-m_{T} regions (R1 and R2) can be used to measure the background shape for the M_J distribution at high m_{T}. A correction factor, near unity, is taken from simulation and is used to account for a possible correlation between M_J and m_{T}.

The observed event yields in the signal regions are consistent with the predictions for the SM background contributions, and exclusion limits are set on the gluino pair production cross sections in the $m_{\tilde{\mathrm{g}}}$-$m_{\tilde{\chi}_1^0}$ plane, as described by the simplified models T1tttt and T5tttt, where the latter is augmented with a model of direct top squark pair production for consistency. In the T1tttt model, gluinos decay via the three-body process $\tilde{\mathrm{g}} \to \mathrm{t\bar{t}}\tilde{\chi}_1^0$, which proceeds via a virtual top squark in the intermediate state. Under the assumption of a 100% branching fraction to this final state, the cross section limit for each model point is compared with the theoretical cross section to determine the excluded particle masses. Gluinos with a mass below 1600 GeV are excluded at a 95% CL for scenarios with low $\tilde{\chi}_1^0$ mass, and neutralinos with a mass below 800 GeV are excluded for a gluino mass of about 1300 GeV. In the T5tttt model, the top squark is lighter than the gluino, which therefore decays via a two-body process. The boundary of the excluded region in the $m_{\tilde{\mathrm{g}}}$-$m_{\tilde{\chi}_1^0}$ plane for T5tttt is found to be only weakly sensitive to the top squark mass. These results significantly extend the sensitivity of single-lepton searches based on data at $\sqrt{s} = 8\,\mathrm{TeV}$.

Acknowledgments

We congratulate our colleagues in the CERN accelerator departments for the excellent performance of the LHC and thank the technical and administrative staffs at CERN and at other CMS institutes for their contributions to the success of the CMS effort. In addition, we gratefully acknowledge the computing centers and personnel of the Worldwide LHC Computing Grid for delivering so effectively the computing infrastructure essential to our analyses. Finally, we acknowledge the enduring support for the construction and operation of the LHC and the CMS detector provided by the following funding agencies: the Austrian Federal Ministry of Science, Research and Economy and the Austrian Science Fund; the Belgian Fonds de la Recherche Scientifique, and Fonds voor Wetenschappelijk Onderzoek; the Brazilian Funding Agencies (CNPq, CAPES, FAPERJ, and FAPESP); the Bulgarian Ministry of Education and Science; CERN; the Chinese Academy of Sciences, Ministry of Science and Technology, and National Natural Science Foundation of China; the Colombian Funding Agency (COLCIENCIAS); the Croatian Ministry of Science, Education and Sport, and the Croatian Science Foundation; the Research Promotion Foundation, Cyprus; the Ministry of Education and Research, Estonian Research Council via IUT23-4 and IUT23-6 and European Regional Development Fund, Estonia; the Academy of Finland, Finnish Ministry of Education and Culture, and Helsinki

Institute of Physics; the Institut National de Physique Nucléaire et de Physique des Particules / CNRS, and Commissariat à l'Énergie Atomique et aux Énergies Alternatives / CEA, France; the Bundesministerium für Bildung und Forschung, Deutsche Forschungsgemeinschaft, and Helmholtz-Gemeinschaft Deutscher Forschungszentren, Germany; the General Secretariat for Research and Technology, Greece; the National Scientific Research Foundation, and National Innovation Office, Hungary; the Department of Atomic Energy and the Department of Science and Technology, India; the Institute for Studies in Theoretical Physics and Mathematics, Iran; the Science Foundation, Ireland; the Istituto Nazionale di Fisica Nucleare, Italy; the Ministry of Science, ICT and Future Planning, and National Research Foundation (NRF), Republic of Korea; the Lithuanian Academy of Sciences; the Ministry of Education, and University of Malaya (Malaysia); the Mexican Funding Agencies (BUAP, CINVESTAV, CONACYT, LNS, SEP, and UASLP-FAI); the Ministry of Business, Innovation and Employment, New Zealand; the Pakistan Atomic Energy Commission; the Ministry of Science and Higher Education and the National Science Centre, Poland; the Fundação para a Ciência e a Tecnologia, Portugal; JINR, Dubna; the Ministry of Education and Science of the Russian Federation, the Federal Agency of Atomic Energy of the Russian Federation, Russian Academy of Sciences, and the Russian Foundation for Basic Research; the Ministry of Education, Science and Technological Development of Serbia; the Secretaría de Estado de Investigación, Desarrollo e Innovación and Programa Consolider-Ingenio 2010, Spain; the Swiss Funding Agencies (ETH Board, ETH Zurich, PSI, SNF, UniZH, Canton Zurich, and SER); the Ministry of Science and Technology, Taipei; the Thailand Center of Excellence in Physics, the Institute for the Promotion of Teaching Science and Technology of Thailand, Special Task Force for Activating Research and the National Science and Technology Development Agency of Thailand; the Scientific and Technical Research Council of Turkey, and Turkish Atomic Energy Authority; the National Academy of Sciences of Ukraine, and State Fund for Fundamental Researches, Ukraine; the Science and Technology Facilities Council, UK; the US Department of Energy, and the US National Science Foundation.

Individuals have received support from the Marie-Curie program and the European Research Council and EPLANET (European Union); the Leventis Foundation; the A. P. Sloan Foundation; the Alexander von Humboldt Foundation; the Belgian Federal Science Policy Office; the Fonds pour la Formation à la Recherche dans l'Industrie et dans l'Agriculture (FRIA-Belgium); the Agentschap voor Innovatie door Wetenschap en Technologie (IWT-Belgium); the Ministry of Education, Youth and Sports (MEYS) of the Czech Republic; the Council of Science and Industrial Research, India; the HOMING PLUS program of the Foundation for Polish Science, cofinanced from European Union, Regional Development Fund; the Mobility Plus program of the Ministry of Science and Higher Education (Poland); the OPUS program of the National Science Center (Poland); the Thalis and Aristeia programs cofinanced by EU-ESF and the Greek NSRF; the National Priorities Research Program by Qatar National Research Fund; the Programa Clarín-COFUND del Principado de Asturias; the Rachadapisek Sompot Fund for Postdoctoral Fellowship, Chulalongkorn University (Thailand); the Chulalongkorn Academic into Its 2nd Century Project Advancement Project (Thailand); and the Welch Foundation, contract C-1845.

References

[1] P. Ramond, "Dual theory for free fermions", *Phys. Rev. D* **3** (1971) 2415, doi:10.1103/PhysRevD.3.2415.

[2] Y. A. Gol'fand and E. P. Likhtman, "Extension of the algebra of Poincaré group generators and violation of P invariance", *JETP Lett.* **13** (1971) 323.

[3] A. Neveu and J. H. Schwarz, "Factorizable dual model of pions", *Nucl. Phys. B* **31** (1971) 86, doi:10.1016/0550-3213(71)90448-2.

[4] D. V. Volkov and V. P. Akulov, "Possible universal neutrino interaction", *JETP Lett.* **16** (1972) 438.

[5] J. Wess and B. Zumino, "A Lagrangian model invariant under supergauge transformations", *Phys. Lett. B* **49** (1974) 52, doi:10.1016/0370-2693(74)90578-4.

[6] J. Wess and B. Zumino, "Supergauge transformations in four dimensions", *Nucl. Phys. B* **70** (1974) 39, doi:10.1016/0550-3213(74)90355-1.

[7] P. Fayet, "Supergauge invariant extension of the Higgs mechanism and a model for the electron and its neutrino", *Nucl. Phys. B* **90** (1975) 104, doi:10.1016/0550-3213(75)90636-7.

[8] H. P. Nilles, "Supersymmetry, supergravity and particle physics", *Phys. Rep.* **110** (1984) 1, doi:10.1016/0370-1573(84)90008-5.

[9] G. 't Hooft, "Naturalness, chiral symmetry, and spontaneous chiral symmetry breaking", in *Recent Developments in Gauge Theories*, G. 't Hooft et al., eds., p. 135. Springer, 1980. NATO Advanced Study Institutes Series B.

[10] E. Witten, "Dynamical breaking of supersymmetry", *Nucl. Phys. B* **188** (1981) 513, doi:10.1016/0550-3213(81)90006-7.

[11] M. Dine, W. Fischler, and M. Srednicki, "Supersymmetric technicolor", *Nucl. Phys. B* **189** (1981) 575, doi:10.1016/0550-3213(81)90582-4.

[12] S. Dimopoulos and S. Raby, "Supercolor", *Nucl. Phys. B* **192** (1981) 353, doi:10.1016/0550-3213(81)90430-2.

[13] S. Dimopoulos and H. Georgi, "Softly broken supersymmetry and SU(5)", *Nucl. Phys. B* **193** (1981) 150, doi:10.1016/0550-3213(81)90522-8.

[14] R. K. Kaul and P. Majumdar, "Cancellation of quadratically divergent mass corrections in globally supersymmetric spontaneously broken gauge theories", *Nucl. Phys. B* **199** (1982) 36, doi:10.1016/0550-3213(82)90565-X.

[15] F. Zwicky, "Die Rotverschiebung von Extragalaktischen Nebeln", *Helv. Phys. Acta* **6** (1933) 110.

[16] V. C. Rubin and W. K. Ford Jr, "Rotation of the Andromeda nebula from a spectroscopic survey of emission regions", *Astrophys. J.* **159** (1970) 379, doi:10.1086/150317.

[17] Particle Data Group, K. A. Olive et al., "Review of Particle Physics", *Chin. Phys. C* **38** (2014) 090001, doi:10.1088/1674-1137/38/9/090001.

[18] S. Dimopoulos, S. Raby, and F. Wilczek, "Supersymmetry and the scale of unification", *Phys. Rev. D* **24** (1981) 1681, doi:10.1103/PhysRevD.24.1681.

[19] N. Sakai, "Naturalness in supersymmetric GUTS", *Z. Phys. C* **11** (1981) 153, doi:10.1007/BF01573998.

[20] L. E. Ibáñez and G. G. Ross, "Low-energy predictions in supersymmetric grand unified theories", *Phys. Lett. B* **105** (1981) 439, doi:10.1016/0370-2693(81)91200-4.

[21] M. B. Einhorn and D. R. T. Jones, "The weak mixing angle and unification mass in supersymmetric SU(5)", *Nucl. Phys. B* **196** (1982) 475, doi:10.1016/0550-3213(82)90502-8.

[22] W. J. Marciano and G. Senjanović, "Predictions of supersymmetric grand unified theories", *Phys. Rev. D* **25** (Jun, 1982) 3092, doi:10.1103/PhysRevD.25.3092.

[23] G. R. Farrar and P. Fayet, "Phenomenology of the production, decay, and detection of new hadronic states associated with supersymmetry", *Phys. Lett. B* **76** (1978) 575, doi:10.1016/0370-2693(78)90858-4.

[24] S. P. Martin, "A Supersymmetry Primer", in *Perspectives on Supersymmetry II*, G. L. Kane, ed., p. 1. 2010. arXiv:hep-ph/9709356. Adv. Ser. Direct. High Energy Phys., vol. 21. doi:10.1142/9789814307505_0001.

[25] ATLAS Collaboration, "Observation of a new particle in the search for the Standard Model Higgs boson with the ATLAS detector at the LHC", *Phys. Lett. B* **716** (2012) 1, doi:10.1016/j.physletb.2012.08.020, arXiv:1207.7214.

[26] CMS Collaboration, "Observation of a new boson at a mass of 125 GeV with the CMS experiment at the LHC", *Phys. Lett. B* **716** (2012) 30, doi:10.1016/j.physletb.2012.08.021, arXiv:1207.7235.

[27] CMS Collaboration, "Observation of a new boson with mass near 125 GeV in pp collisions at $\sqrt{s}$ = 7 and 8 TeV", *JHEP* **06** (2013) 081, doi:10.1007/JHEP06(2013)081, arXiv:1303.4571.

[28] CMS Collaboration, "Precise determination of the mass of the Higgs boson and tests of compatibility of its couplings with the standard model predictions using proton collisions at 7 and 8 TeV", *Eur. Phys. J. C* **75** (2015) 212, doi:10.1140/epjc/s10052-015-3351-7, arXiv:1412.8662.

[29] ATLAS Collaboration, "Measurement of the Higgs boson mass from the $H \to \gamma\gamma$ and $H \to ZZ^* \to 4\ell$ channels with the ATLAS detector using 25 fb^{-1} of pp collision data", *Phys. Rev. D* **90** (2014) 052004, doi:10.1103/PhysRevD.90.052004, arXiv:1406.3827.

[30] ATLAS and CMS Collaborations, "Combined measurement of the Higgs boson mass in pp collisions at $\sqrt{s} = 7$ and 8 TeV with the ATLAS and CMS experiments", *Phys. Rev. Lett.* **114** (2015) 191803, doi:10.1103/PhysRevLett.114.191803, arXiv:1503.07589.

[31] S. Dimopoulos and G. F. Giudice, "Naturalness constraints in supersymmetric theories with nonuniversal soft terms", *Phys. Lett. B* **357** (1995) 573, doi:10.1016/0370-2693(95)00961-J, arXiv:hep-ph/9507282.

[32] R. Barbieri and D. Pappadopulo, "S-particles at their naturalness limits", *JHEP* **10** (2009) 061, doi:10.1088/1126-6708/2009/10/061, arXiv:0906.4546.

[33] M. Papucci, J. T. Ruderman, and A. Weiler, "Natural SUSY endures", *JHEP* **09** (2012) 035, doi:10.1007/JHEP09(2012)035, arXiv:1110.6926.

[34] J. L. Feng, "Naturalness and the status of supersymmetry", *Ann. Rev. Nucl. Part. Sci.* **63** (2013) 351, doi:10.1146/annurev-nucl-102010-130447, arXiv:1302.6587.

[35] N. Craig, "The state of supersymmetry after Run I of the LHC", in *Beyond the Standard Model after the first run of the LHC, Arcetri, Florence, Italy, May 20-July 12, 2013*. 2013. arXiv:1309.0528.

[36] ATLAS Collaboration, "Search for strong production of supersymmetric particles in final states with missing transverse momentum and at least three b-jets at $\sqrt{s}$= 8 TeV proton-proton collisions with the ATLAS detector", *JHEP* **10** (2014) 024, doi:10.1007/JHEP10(2014)024, arXiv:1407.0600.

[37] ATLAS Collaboration, "Search for squarks and gluinos in events with isolated leptons, jets and missing transverse momentum at $\sqrt{s} = 8$ TeV with the ATLAS detector", *JHEP* **04** (2015) 116, doi:10.1007/JHEP04(2015)116, arXiv:1501.03555.

[38] CMS Collaboration, "Search for supersymmetry in pp collisions at $\sqrt{s} = 8$ TeV in events with a single lepton, large jet multiplicity, and multiple b jets", *Phys. Lett. B* **733** (2014) 328, doi:10.1016/j.physletb.2014.04.023, arXiv:1311.4937.

[39] C. Borschensky et al., "Squark and gluino production cross sections in pp collisions at $\sqrt{s} = 13$, 14, 33 and 100 TeV", *Eur. Phys. J. C* **74** (2014) 3174, doi:10.1140/epjc/s10052-014-3174-y, arXiv:1407.5066.

[40] M. Czakon, P. Fiedler, and A. Mitov, "The total top quark pair production cross-section at $\mathcal{O}(\alpha_S^4)$", *Phys. Rev. Lett.* **110** (2013) 252004, doi:10.1103/PhysRevLett.110.252004, arXiv:1303.6254.

[41] CMS Collaboration, "Interpretation of searches for supersymmetry with simplified models", *Phys. Rev. D* **88** (2013) 052017, doi:10.1103/PhysRevD.88.052017, arXiv:1301.2175.

[42] J. Alwall, P. Schuster, and N. Toro, "Simplified models for a first characterization of new physics at the LHC", *Phys. Rev. D* **79** (2009) 075020, doi:10.1103/PhysRevD.79.075020, arXiv:0810.3921.

[43] J. Alwall, M.-P. Le, M. Lisanti, and J. G. Wacker, "Model-independent jets plus missing energy searches", *Phys. Rev. D* **79** (2009) 015005, doi:10.1103/PhysRevD.79.015005, arXiv:0809.3264.

[44] D. Alves et al., "Simplified models for LHC new physics searches", *J. Phys. G* **39** (2012) 105005, doi:10.1088/0954-3899/39/10/105005, arXiv:1105.2838.

[45] A. Hook, E. Izaguirre, M. Lisanti, and J. G. Wacker, "High multiplicity searches at the LHC using jet masses", *Phys. Rev. D* **85** (2012) 055029, doi:10.1103/PhysRevD.85.055029, arXiv:1202.0558.

[46] T. Cohen, E. Izaguirre, M. Lisanti, and H. K. Lou, "Jet substructure by accident", *JHEP* **03** (2013) 161, doi:10.1007/JHEP03(2013)161, arXiv:1212.1456.

[47] S. El Hedri, A. Hook, M. Jankowiak, and J. G. Wacker, "Learning how to count: a high multiplicity search for the LHC", *JHEP* **08** (2013) 136, doi:10.1007/JHEP08(2013)136, arXiv:1302.1870.

[48] ATLAS Collaboration, "Search for massive supersymmetric particles decaying to many jets using the ATLAS detector in pp collisions at $\sqrt{s} = 8$ TeV", *Phys. Rev. D* **91** (2015) 112016, doi:10.1103/PhysRevD.91.112016, arXiv:1502.05686.

[49] ATLAS Collaboration, "Search for new phenomena in final states with large jet multiplicities and missing transverse momentum at $\sqrt{s} = 8$ TeV proton-proton collisions using the ATLAS experiment", *JHEP* **10** (2013) 130, doi:10.1007/JHEP10(2013)130, arXiv:1308.1841. [Erratum: doi:10.1007/JHEP01(2014)109].

[50] CMS Collaboration, "Commissioning the performance of key observables used in SUSY searches with the first 13 TeV data", CMS Detector Performance Report CMS-DP-2015-035, CERN, 2015.

[51] CMS Collaboration, "The CMS experiment at the CERN LHC", *JINST* **3** (2008) S08004, doi:10.1088/1748-0221/3/08/S08004.

[52] J. Alwall et al., "The automated computation of tree-level and next-to-leading order differential cross sections, and their matching to parton shower simulations", *JHEP* **07** (2014) 079, doi:10.1007/JHEP07(2014)079, arXiv:1405.0301.

[53] S. Alioli, P. Nason, C. Oleari, and E. Re, "NLO single-top production matched with shower in POWHEG: s- and t-channel contributions", *JHEP* **09** (2009) 111, doi:10.1088/1126-6708/2009/09/111, arXiv:0907.4076. [Erratum: doi:10.1007/JHEP02(2010)011].

[54] E. Re, "Single-top Wt-channel production matched with parton showers using the POWHEG method", *Eur. Phys. J. C* **71** (2011) 1547, doi:10.1140/epjc/s10052-011-1547-z, arXiv:1009.2450.

[55] NNPDF Collaboration, "Parton distributions for the LHC Run II", *JHEP* **04** (2015) 040, doi:10.1007/JHEP04(2015)040, arXiv:1410.8849.

[56] T. Sjöstrand et al., "An Introduction to PYTHIA 8.2", *Comput. Phys. Commun.* **191** (2015) 159, doi:10.1016/j.cpc.2015.01.024, arXiv:1410.3012.

[57] CMS Collaboration, "Event generator tunes obtained from underlying event and multiparton scattering measurements", *Eur. Phys. J. C* **76** (2016), no. 3, 155, doi:10.1140/epjc/s10052-016-3988-x, arXiv:1512.00815.

[58] GEANT4 Collaboration, "GEANT4—a simulation toolkit", *Nucl. Instrum. Meth. A* **506** (2003) 250, doi:10.1016/S0168-9002(03)01368-8.

[59] CMS Collaboration, "Measurement of the differential cross section for top quark pair production in pp collisions at $\sqrt{s} = 8$ TeV", *Eur. Phys. J. C* **75** (2015) 542, doi:10.1140/epjc/s10052-015-3709-x, arXiv:1505.04480.

[60] CMS Collaboration, "The fast simulation of the CMS detector at LHC", *J. Phys. Conf. Ser.* **331** (2011) 032049, doi:10.1088/1742-6596/331/3/032049.

[61] W. Beenakker, R. Hopker, M. Spira, and P. M. Zerwas, "Squark and gluino production at hadron colliders", *Nucl. Phys. B* **492** (1997) 51, doi:10.1016/S0550-3213(97)00084-9, arXiv:hep-ph/9610490.

[62] A. Kulesza and L. Motyka, "Threshold resummation for squark-antisquark and gluino-pair production at the LHC", *Phys. Rev. Lett.* **102** (2009) 111802, doi:10.1103/PhysRevLett.102.111802, arXiv:0807.2405.

[63] A. Kulesza and L. Motyka, "Soft gluon resummation for the production of gluino-gluino and squark-antisquark pairs at the LHC", *Phys. Rev. D* **80** (2009) 095004, doi:10.1103/PhysRevD.80.095004, arXiv:0905.4749.

[64] W. Beenakker et al., "Soft-gluon resummation for squark and gluino hadroproduction", *JHEP* **12** (2009) 041, doi:10.1088/1126-6708/2009/12/041, arXiv:0909.4418.

[65] CMS Collaboration, "Particle flow event reconstruction in CMS and performance for jets, taus and $E_{\mathrm{T}}^{\mathrm{miss}}$", CMS Physics Analysis Summary CMS-PAS-PFT-09-001, CERN, 2009.

[66] CMS Collaboration, "Commissioning of the particle-flow event reconstruction with the first LHC collisions recorded in the CMS detector", CMS Physics Analysis Summary CMS-PAS-PFT-10-001, CERN, 2010.

[67] M. Cacciari, G. P. Salam, and G. Soyez, "The anti-k_{t} jet clustering algorithm", *JHEP* **04** (2008) 063, doi:10.1088/1126-6708/2008/04/063, arXiv:0802.1189.

[68] M. Cacciari, G. P. Salam, and G. Soyez, "FastJet user manual", *Eur. Phys. J. C* **72** (2012) 1896, doi:10.1140/epjc/s10052-012-1896-2, arXiv:1111.6097.

[69] M. Cacciari and G. P. Salam, "Pileup subtraction using jet areas", *Phys. Lett. B* **659** (2008) 119, doi:10.1016/j.physletb.2007.09.077, arXiv:0707.1378.

[70] CMS Collaboration, "Determination of jet energy calibration and transverse momentum resolution in CMS", *JINST* **6** (2011) P11002, doi:10.1088/1748-0221/6/11/P11002, arXiv:1107.4277.

[71] CMS Collaboration, "Identification of b-quark jets with the CMS experiment", *JINST* **8** (2013) P04013, doi:10.1088/1748-0221/8/04/P04013, arXiv:1211.4462.

[72] CMS Collaboration, "Identification of b quark jets at the CMS Experiment in the LHC Run 2", CMS Physics Analysis Summary CMS-PAS-BTV-15-001, CERN, 2016.

[73] CMS Collaboration, "Performance of electron reconstruction and selection with the CMS detector in proton-proton collisions at $\sqrt{s} = 8\,\mathrm{TeV}$", *JINST* **10** (2015) P06005, doi:10.1088/1748-0221/10/06/P06005, arXiv:1502.02701.

[74] CMS Collaboration, "Performance of CMS muon reconstruction in pp collision events at $\sqrt{s} = 7\,\mathrm{TeV}$", *JINST* **7** (2012) P10002, doi:10.1088/1748-0221/7/10/P10002, arXiv:1206.4071.

[75] K. Rehermann and B. Tweedie, "Efficient identification of boosted semileptonic top quarks at the LHC", *JHEP* **03** (2011) 059, doi:10.1007/JHEP03(2011)059, arXiv:1007.2221.

[76] ATLAS Collaboration, "Search for direct pair production of the top squark in all-hadronic final states in proton-proton collisions at $\sqrt{s} = 8\,\mathrm{TeV}$ with the ATLAS detector", *JHEP* **09** (2014) 015, doi:10.1007/JHEP09(2014)015, arXiv:1406.1122.

[77] CMS Collaboration, "Search for supersymmetry in the multijet and missing transverse momentum final state in pp collisions at 13 TeV", (2016). arXiv:1602.06581. Submitted to Phys. Lett. B.

[78] CMS Collaboration, "CMS luminosity measurement for the 2015 data taking period", CMS Physics Analysis Summary CMS-PAS-LUM-15-001, CERN, Geneva, 2016.

[79] T. Junk, "Confidence level computation for combining searches with small statistics", *Nucl. Instrum. Meth. A* **434** (1999) 435, doi:10.1016/S0168-9002(99)00498-2, arXiv:hep-ex/9902006.

[80] A. L. Read, "Presentation of search results: the CL_s technique", *J. Phys. G* **28** (2002) 2693, doi:10.1088/0954-3899/28/10/313.

[81] ATLAS Collaboration, CMS Collaboration, LHC Higgs Combination Group, "Procedure for the LHC Higgs boson search combination in Summer 2011", Technical Report CMS-NOTE-2011-005, ATL-PHYS-PUB-2011-11, CERN, 2011.

A The CMS Collaboration

Yerevan Physics Institute, Yerevan, Armenia
V. Khachatryan, A.M. Sirunyan, A. Tumasyan

Institut für Hochenergiephysik der OeAW, Wien, Austria
W. Adam, E. Asilar, T. Bergauer, J. Brandstetter, E. Brondolin, M. Dragicevic, J. Erö, M. Flechl, M. Friedl, R. Frühwirth[1], V.M. Ghete, C. Hartl, N. Hörmann, J. Hrubec, M. Jeitler[1], A. König, I. Krätschmer, D. Liko, T. Matsushita, I. Mikulec, D. Rabady, N. Rad, B. Rahbaran, H. Rohringer, J. Schieck[1], J. Strauss, W. Treberer-Treberspurg, W. Waltenberger, C.-E. Wulz[1]

National Centre for Particle and High Energy Physics, Minsk, Belarus
V. Mossolov, N. Shumeiko, J. Suarez Gonzalez

Universiteit Antwerpen, Antwerpen, Belgium
S. Alderweireldt, E.A. De Wolf, X. Janssen, J. Lauwers, M. Van De Klundert, H. Van Haevermaet, P. Van Mechelen, N. Van Remortel, A. Van Spilbeeck

Vrije Universiteit Brussel, Brussel, Belgium
S. Abu Zeid, F. Blekman, J. D'Hondt, N. Daci, I. De Bruyn, K. Deroover, N. Heracleous, S. Lowette, S. Moortgat, L. Moreels, A. Olbrechts, Q. Python, S. Tavernier, W. Van Doninck, P. Van Mulders, I. Van Parijs

Université Libre de Bruxelles, Bruxelles, Belgium
H. Brun, C. Caillol, B. Clerbaux, G. De Lentdecker, H. Delannoy, G. Fasanella, L. Favart, R. Goldouzian, A. Grebenyuk, G. Karapostoli, T. Lenzi, A. Léonard, J. Luetic, T. Maerschalk, A. Marinov, A. Randle-conde, T. Seva, C. Vander Velde, P. Vanlaer, R. Yonamine, F. Zenoni, F. Zhang[2]

Ghent University, Ghent, Belgium
A. Cimmino, T. Cornelis, D. Dobur, A. Fagot, G. Garcia, M. Gul, D. Poyraz, S. Salva, R. Schöfbeck, M. Tytgat, W. Van Driessche, E. Yazgan, N. Zaganidis

Université Catholique de Louvain, Louvain-la-Neuve, Belgium
C. Beluffi[3], O. Bondu, S. Brochet, G. Bruno, A. Caudron, L. Ceard, S. De Visscher, C. Delaere, M. Delcourt, L. Forthomme, B. Francois, A. Giammanco, A. Jafari, P. Jez, M. Komm, V. Lemaitre, A. Magitteri, A. Mertens, M. Musich, C. Nuttens, K. Piotrzkowski, L. Quertenmont, M. Selvaggi, M. Vidal Marono, S. Wertz

Université de Mons, Mons, Belgium
N. Beliy

Centro Brasileiro de Pesquisas Fisicas, Rio de Janeiro, Brazil
W.L. Aldá Júnior, F.L. Alves, G.A. Alves, L. Brito, C. Hensel, A. Moraes, M.E. Pol, P. Rebello Teles

Universidade do Estado do Rio de Janeiro, Rio de Janeiro, Brazil
E. Belchior Batista Das Chagas, W. Carvalho, J. Chinellato[4], A. Custódio, E.M. Da Costa, G.G. Da Silveira, D. De Jesus Damiao, C. De Oliveira Martins, S. Fonseca De Souza, L.M. Huertas Guativa, H. Malbouisson, D. Matos Figueiredo, C. Mora Herrera, L. Mundim, H. Nogima, W.L. Prado Da Silva, A. Santoro, A. Sznajder, E.J. Tonelli Manganote[4], A. Vilela Pereira

Universidade Estadual Paulista [a], Universidade Federal do ABC [b], São Paulo, Brazil
S. Ahuja[a], C.A. Bernardes[b], S. Dogra[a], T.R. Fernandez Perez Tomei[a], E.M. Gregores[b],

P.G. Mercadante[b], C.S. Moon[a,5], S.F. Novaes[a], Sandra S. Padula[a], D. Romero Abad[b], J.C. Ruiz Vargas

Institute for Nuclear Research and Nuclear Energy, Sofia, Bulgaria
A. Aleksandrov, R. Hadjiiska, P. Iaydjiev, M. Rodozov, S. Stoykova, G. Sultanov, M. Vutova

University of Sofia, Sofia, Bulgaria
A. Dimitrov, I. Glushkov, L. Litov, B. Pavlov, P. Petkov

Beihang University, Beijing, China
W. Fang[6]

Institute of High Energy Physics, Beijing, China
M. Ahmad, J.G. Bian, G.M. Chen, H.S. Chen, M. Chen, Y. Chen[7], T. Cheng, C.H. Jiang, D. Leggat, Z. Liu, F. Romeo, S.M. Shaheen, A. Spiezia, J. Tao, C. Wang, Z. Wang, H. Zhang, J. Zhao

State Key Laboratory of Nuclear Physics and Technology, Peking University, Beijing, China
Y. Ban, Q. Li, S. Liu, Y. Mao, S.J. Qian, D. Wang, Z. Xu

Universidad de Los Andes, Bogota, Colombia
C. Avila, A. Cabrera, L.F. Chaparro Sierra, C. Florez, J.P. Gomez, C.F. González Hernández, J.D. Ruiz Alvarez, J.C. Sanabria

University of Split, Faculty of Electrical Engineering, Mechanical Engineering and Naval Architecture, Split, Croatia
N. Godinovic, D. Lelas, I. Puljak, P.M. Ribeiro Cipriano

University of Split, Faculty of Science, Split, Croatia
Z. Antunovic, M. Kovac

Institute Rudjer Boskovic, Zagreb, Croatia
V. Brigljevic, D. Ferencek, K. Kadija, S. Micanovic, L. Sudic

University of Cyprus, Nicosia, Cyprus
A. Attikis, G. Mavromanolakis, J. Mousa, C. Nicolaou, F. Ptochos, P.A. Razis, H. Rykaczewski

Charles University, Prague, Czech Republic
M. Finger[8], M. Finger Jr.[8]

Universidad San Francisco de Quito, Quito, Ecuador
E. Carrera Jarrin

Academy of Scientific Research and Technology of the Arab Republic of Egypt, Egyptian Network of High Energy Physics, Cairo, Egypt
A.A. Abdelalim[9,10], E. El-khateeb[11,11], M.A. Mahmoud[12,13], A. Radi[13,11]

National Institute of Chemical Physics and Biophysics, Tallinn, Estonia
B. Calpas, M. Kadastik, M. Murumaa, L. Perrini, M. Raidal, A. Tiko, C. Veelken

Department of Physics, University of Helsinki, Helsinki, Finland
P. Eerola, J. Pekkanen, M. Voutilainen

Helsinki Institute of Physics, Helsinki, Finland
J. Härkönen, V. Karimäki, R. Kinnunen, T. Lampén, K. Lassila-Perini, S. Lehti, T. Lindén, P. Luukka, T. Peltola, J. Tuominiemi, E. Tuovinen, L. Wendland

Lappeenranta University of Technology, Lappeenranta, Finland
J. Talvitie, T. Tuuva

DSM/IRFU, CEA/Saclay, Gif-sur-Yvette, France
M. Besancon, F. Couderc, M. Dejardin, D. Denegri, B. Fabbro, J.L. Faure, C. Favaro, F. Ferri, S. Ganjour, S. Ghosh, A. Givernaud, P. Gras, G. Hamel de Monchenault, P. Jarry, I. Kucher, E. Locci, M. Machet, J. Malcles, J. Rander, A. Rosowsky, M. Titov, A. Zghiche

Laboratoire Leprince-Ringuet, Ecole Polytechnique, IN2P3-CNRS, Palaiseau, France
A. Abdulsalam, I. Antropov, S. Baffioni, F. Beaudette, P. Busson, L. Cadamuro, E. Chapon, C. Charlot, O. Davignon, R. Granier de Cassagnac, M. Jo, S. Lisniak, P. Miné, I.N. Naranjo, M. Nguyen, C. Ochando, G. Ortona, P. Paganini, P. Pigard, S. Regnard, R. Salerno, Y. Sirois, T. Strebler, Y. Yilmaz, A. Zabi

Institut Pluridisciplinaire Hubert Curien, Université de Strasbourg, Université de Haute Alsace Mulhouse, CNRS/IN2P3, Strasbourg, France
J.-L. Agram[14], J. Andrea, A. Aubin, D. Bloch, J.-M. Brom, M. Buttignol, E.C. Chabert, N. Chanon, C. Collard, E. Conte[14], X. Coubez, J.-C. Fontaine[14], D. Gelé, U. Goerlach, A.-C. Le Bihan, J.A. Merlin[15], K. Skovpen, P. Van Hove

Centre de Calcul de l'Institut National de Physique Nucleaire et de Physique des Particules, CNRS/IN2P3, Villeurbanne, France
S. Gadrat

Université de Lyon, Université Claude Bernard Lyon 1, CNRS-IN2P3, Institut de Physique Nucléaire de Lyon, Villeurbanne, France
S. Beauceron, C. Bernet, G. Boudoul, E. Bouvier, C.A. Carrillo Montoya, R. Chierici, D. Contardo, B. Courbon, P. Depasse, H. El Mamouni, J. Fan, J. Fay, S. Gascon, M. Gouzevitch, G. Grenier, B. Ille, F. Lagarde, I.B. Laktineh, M. Lethuillier, L. Mirabito, A.L. Pequegnot, S. Perries, A. Popov[16], D. Sabes, V. Sordini, M. Vander Donckt, P. Verdier, S. Viret

Georgian Technical University, Tbilisi, Georgia
A. Khvedelidze[8]

Tbilisi State University, Tbilisi, Georgia
Z. Tsamalaidze[8]

RWTH Aachen University, I. Physikalisches Institut, Aachen, Germany
C. Autermann, S. Beranek, L. Feld, A. Heister, M.K. Kiesel, K. Klein, M. Lipinski, A. Ostapchuk, M. Preuten, F. Raupach, S. Schael, C. Schomakers, J.F. Schulte, J. Schulz, T. Verlage, H. Weber, V. Zhukov[16]

RWTH Aachen University, III. Physikalisches Institut A, Aachen, Germany
M. Brodski, E. Dietz-Laursonn, D. Duchardt, M. Endres, M. Erdmann, S. Erdweg, T. Esch, R. Fischer, A. Güth, T. Hebbeker, C. Heidemann, K. Hoepfner, S. Knutzen, M. Merschmeyer, A. Meyer, P. Millet, S. Mukherjee, M. Olschewski, K. Padeken, P. Papacz, T. Pook, M. Radziej, H. Reithler, M. Rieger, F. Scheuch, L. Sonnenschein, D. Teyssier, S. Thüer

RWTH Aachen University, III. Physikalisches Institut B, Aachen, Germany
V. Cherepanov, Y. Erdogan, G. Flügge, F. Hoehle, B. Kargoll, T. Kress, A. Künsken, J. Lingemann, A. Nehrkorn, A. Nowack, I.M. Nugent, C. Pistone, O. Pooth, A. Stahl[15]

Deutsches Elektronen-Synchrotron, Hamburg, Germany
M. Aldaya Martin, C. Asawatangtrakuldee, I. Asin, K. Beernaert, O. Behnke, U. Behrens, A.A. Bin Anuar, K. Borras[17], A. Campbell, P. Connor, C. Contreras-Campana, F. Costanza,

C. Diez Pardos, G. Dolinska, G. Eckerlin, D. Eckstein, E. Gallo[18], J. Garay Garcia, A. Geiser, A. Gizhko, J.M. Grados Luyando, P. Gunnellini, A. Harb, J. Hauk, M. Hempel[19], H. Jung, A. Kalogeropoulos, O. Karacheban[19], M. Kasemann, J. Keaveney, J. Kieseler, C. Kleinwort, I. Korol, W. Lange, A. Lelek, J. Leonard, K. Lipka, A. Lobanov, W. Lohmann[19], R. Mankel, I.-A. Melzer-Pellmann, A.B. Meyer, G. Mittag, J. Mnich, A. Mussgiller, E. Ntomari, D. Pitzl, R. Placakyte, A. Raspereza, B. Roland, M.Ö. Sahin, P. Saxena, T. Schoerner-Sadenius, C. Seitz, S. Spannagel, N. Stefaniuk, K.D. Trippkewitz, G.P. Van Onsem, R. Walsh, C. Wissing

University of Hamburg, Hamburg, Germany
V. Blobel, M. Centis Vignali, A.R. Draeger, T. Dreyer, E. Garutti, K. Goebel, D. Gonzalez, J. Haller, M. Hoffmann, A. Junkes, R. Klanner, R. Kogler, N. Kovalchuk, T. Lapsien, T. Lenz, I. Marchesini, D. Marconi, M. Meyer, M. Niedziela, D. Nowatschin, J. Ott, F. Pantaleo[15], T. Peiffer, A. Perieanu, J. Poehlsen, C. Sander, C. Scharf, P. Schleper, A. Schmidt, S. Schumann, J. Schwandt, H. Stadie, G. Steinbrück, F.M. Stober, M. Stöver, H. Tholen, D. Troendle, E. Usai, L. Vanelderen, A. Vanhoefer, B. Vormwald

Institut für Experimentelle Kernphysik, Karlsruhe, Germany
C. Barth, C. Baus, J. Berger, E. Butz, T. Chwalek, F. Colombo, W. De Boer, A. Dierlamm, S. Fink, R. Friese, M. Giffels, A. Gilbert, D. Haitz, F. Hartmann[15], S.M. Heindl, U. Husemann, I. Katkov[16], P. Lobelle Pardo, B. Maier, H. Mildner, M.U. Mozer, T. Müller, Th. Müller, M. Plagge, G. Quast, K. Rabbertz, S. Röcker, F. Roscher, M. Schröder, G. Sieber, H.J. Simonis, R. Ulrich, J. Wagner-Kuhr, S. Wayand, M. Weber, T. Weiler, S. Williamson, C. Wöhrmann, R. Wolf

Institute of Nuclear and Particle Physics (INPP), NCSR Demokritos, Aghia Paraskevi, Greece
G. Anagnostou, G. Daskalakis, T. Geralis, V.A. Giakoumopoulou, A. Kyriakis, D. Loukas, I. Topsis-Giotis

National and Kapodistrian University of Athens, Athens, Greece
A. Agapitos, S. Kesisoglou, A. Panagiotou, N. Saoulidou, E. Tziaferi

University of Ioánnina, Ioánnina, Greece
I. Evangelou, G. Flouris, C. Foudas, P. Kokkas, N. Loukas, N. Manthos, I. Papadopoulos, E. Paradas

MTA-ELTE Lendület CMS Particle and Nuclear Physics Group, Eötvös Loránd University
N. Filipovic

Wigner Research Centre for Physics, Budapest, Hungary
G. Bencze, C. Hajdu, P. Hidas, D. Horvath[20], F. Sikler, V. Veszpremi, G. Vesztergombi[21], A.J. Zsigmond

Institute of Nuclear Research ATOMKI, Debrecen, Hungary
N. Beni, S. Czellar, J. Karancsi[22], A. Makovec, J. Molnar, Z. Szillasi

University of Debrecen, Debrecen, Hungary
M. Bartók[21], P. Raics, Z.L. Trocsanyi, B. Ujvari

National Institute of Science Education and Research, Bhubaneswar, India
S. Bahinipati, S. Choudhury[23], P. Mal, K. Mandal, A. Nayak[24], D.K. Sahoo, N. Sahoo, S.K. Swain

Panjab University, Chandigarh, India
S. Bansal, S.B. Beri, V. Bhatnagar, R. Chawla, R. Gupta, U.Bhawandeep, A.K. Kalsi, A. Kaur, M. Kaur, R. Kumar, A. Mehta, M. Mittal, J.B. Singh, G. Walia

University of Delhi, Delhi, India
Ashok Kumar, A. Bhardwaj, B.C. Choudhary, R.B. Garg, S. Keshri, A. Kumar, S. Malhotra, M. Naimuddin, N. Nishu, K. Ranjan, R. Sharma, V. Sharma

Saha Institute of Nuclear Physics, Kolkata, India
R. Bhattacharya, S. Bhattacharya, K. Chatterjee, S. Dey, S. Dutt, S. Dutta, S. Ghosh, N. Majumdar, A. Modak, K. Mondal, S. Mukhopadhyay, S. Nandan, A. Purohit, A. Roy, D. Roy, S. Roy Chowdhury, S. Sarkar, M. Sharan, S. Thakur

Indian Institute of Technology Madras, Madras, India
P.K. Behera

Bhabha Atomic Research Centre, Mumbai, India
R. Chudasama, D. Dutta, V. Jha, V. Kumar, A.K. Mohanty[15], P.K. Netrakanti, L.M. Pant, P. Shukla, A. Topkar

Tata Institute of Fundamental Research-A, Mumbai, India
T. Aziz, S. Dugad, G. Kole, B. Mahakud, S. Mitra, G.B. Mohanty, N. Sur, B. Sutar

Tata Institute of Fundamental Research-B, Mumbai, India
S. Banerjee, S. Bhowmik[25], R.K. Dewanjee, S. Ganguly, M. Guchait, Sa. Jain, S. Kumar, M. Maity[25], G. Majumder, K. Mazumdar, B. Parida, T. Sarkar[25], N. Wickramage[26]

Indian Institute of Science Education and Research (IISER), Pune, India
S. Chauhan, S. Dube, A. Kapoor, K. Kothekar, A. Rane, S. Sharma

Institute for Research in Fundamental Sciences (IPM), Tehran, Iran
H. Bakhshiansohi, H. Behnamian, S. Chenarani[27], E. Eskandari Tadavani, S.M. Etesami[27], A. Fahim[28], M. Khakzad, M. Mohammadi Najafabadi, M. Naseri, S. Paktinat Mehdiabadi, F. Rezaei Hosseinabadi, B. Safarzadeh[29], M. Zeinali

University College Dublin, Dublin, Ireland
M. Felcini, M. Grunewald

INFN Sezione di Bari [a], Università di Bari [b], Politecnico di Bari [c], Bari, Italy
M. Abbrescia[a,b], C. Calabria[a,b], C. Caputo[a,b], A. Colaleo[a], D. Creanza[a,c], L. Cristella[a,b], N. De Filippis[a,c], M. De Palma[a,b], L. Fiore[a], G. Iaselli[a,c], G. Maggi[a,c], M. Maggi[a], G. Miniello[a,b], S. My[a,b], S. Nuzzo[a,b], A. Pompili[a,b], G. Pugliese[a,c], R. Radogna[a,b], A. Ranieri[a], G. Selvaggi[a,b], L. Silvestris[a,15], R. Venditti[a,b], P. Verwilligen[a]

INFN Sezione di Bologna [a], Università di Bologna [b], Bologna, Italy
G. Abbiendi[a], C. Battilana, D. Bonacorsi[a,b], S. Braibant-Giacomelli[a,b], L. Brigliadori[a,b], R. Campanini[a,b], P. Capiluppi[a,b], A. Castro[a,b], F.R. Cavallo[a], S.S. Chhibra[a,b], G. Codispoti[a,b], M. Cuffiani[a,b], G.M. Dallavalle[a], F. Fabbri[a], A. Fanfani[a,b], D. Fasanella[a,b], P. Giacomelli[a], C. Grandi[a], L. Guiducci[a,b], S. Marcellini[a], G. Masetti[a], A. Montanari[a], F.L. Navarria[a,b], A. Perrotta[a], A.M. Rossi[a,b], T. Rovelli[a,b], G.P. Siroli[a,b], N. Tosi[a,b,15]

INFN Sezione di Catania [a], Università di Catania [b], Catania, Italy
S. Albergo[a,b], M. Chiorboli[a,b], S. Costa[a,b], A. Di Mattia[a], F. Giordano[a,b], R. Potenza[a,b], A. Tricomi[a,b], C. Tuve[a,b]

INFN Sezione di Firenze [a], Università di Firenze [b], Firenze, Italy
G. Barbagli[a], V. Ciulli[a,b], C. Civinini[a], R. D'Alessandro[a,b], E. Focardi[a,b], V. Gori[a,b], P. Lenzi[a,b], M. Meschini[a], S. Paoletti[a], G. Sguazzoni[a], L. Viliani[a,b,15]

INFN Laboratori Nazionali di Frascati, Frascati, Italy
L. Benussi, S. Bianco, F. Fabbri, D. Piccolo, F. Primavera[15]

INFN Sezione di Genova [a], Università di Genova [b], Genova, Italy
V. Calvelli[a,b], F. Ferro[a], M. Lo Vetere[a,b], M.R. Monge[a,b], E. Robutti[a], S. Tosi[a,b]

INFN Sezione di Milano-Bicocca [a], Università di Milano-Bicocca [b], Milano, Italy
L. Brianza, M.E. Dinardo[a,b], S. Fiorendi[a,b], S. Gennai[a], A. Ghezzi[a,b], P. Govoni[a,b], S. Malvezzi[a], R.A. Manzoni[a,b,15], B. Marzocchi[a,b], D. Menasce[a], L. Moroni[a], M. Paganoni[a,b], D. Pedrini[a], S. Pigazzini, S. Ragazzi[a,b], T. Tabarelli de Fatis[a,b]

INFN Sezione di Napoli [a], Università di Napoli 'Federico II' [b], Napoli, Italy, Università della Basilicata [c], Potenza, Italy, Università G. Marconi [d], Roma, Italy
S. Buontempo[a], N. Cavallo[a,c], G. De Nardo, S. Di Guida[a,d,15], M. Esposito[a,b], F. Fabozzi[a,c], A.O.M. Iorio[a,b], G. Lanza[a], L. Lista[a], S. Meola[a,d,15], M. Merola[a], P. Paolucci[a,15], C. Sciacca[a,b], F. Thyssen

INFN Sezione di Padova [a], Università di Padova [b], Padova, Italy, Università di Trento [c], Trento, Italy
P. Azzi[a,15], L. Benato[a,b], D. Bisello[a,b], A. Boletti[a,b], R. Carlin[a,b], A. Carvalho Antunes De Oliveira[a,b], P. Checchia[a], M. Dall'Osso[a,b], P. De Castro Manzano[a], T. Dorigo[a], U. Dosselli[a], F. Gasparini[a,b], F. Gonella[a], S. Lacaprara[a], M. Margoni[a,b], A.T. Meneguzzo[a,b], J. Pazzini[a,b,15], M. Pegoraro[a], N. Pozzobon[a,b], P. Ronchese[a,b], M. Sgaravatto[a], F. Simonetto[a,b], E. Torassa[a], M. Zanetti, P. Zotto[a,b], A. Zucchetta[a,b], G. Zumerle[a,b]

INFN Sezione di Pavia [a], Università di Pavia [b], Pavia, Italy
A. Braghieri[a], A. Magnani[a,b], P. Montagna[a,b], S.P. Ratti[a,b], V. Re[a], C. Riccardi[a,b], P. Salvini[a], I. Vai[a,b], P. Vitulo[a,b]

INFN Sezione di Perugia [a], Università di Perugia [b], Perugia, Italy
L. Alunni Solestizi[a,b], G.M. Bilei[a], D. Ciangottini[a,b], L. Fanò[a,b], P. Lariccia[a,b], R. Leonardi[a,b], G. Mantovani[a,b], M. Menichelli[a], A. Saha[a], A. Santocchia[a,b]

INFN Sezione di Pisa [a], Università di Pisa [b], Scuola Normale Superiore di Pisa [c], Pisa, Italy
K. Androsov[a,30], P. Azzurri[a,15], G. Bagliesi[a], J. Bernardini[a], T. Boccali[a], R. Castaldi[a], M.A. Ciocci[a,30], R. Dell'Orso[a], S. Donato[a,c], G. Fedi, A. Giassi[a], M.T. Grippo[a,30], F. Ligabue[a,c], T. Lomtadze[a], L. Martini[a,b], A. Messineo[a,b], F. Palla[a], A. Rizzi[a,b], A. Savoy-Navarro[a,31], P. Spagnolo[a], R. Tenchini[a], G. Tonelli[a,b], A. Venturi[a], P.G. Verdini[a]

INFN Sezione di Roma [a], Università di Roma [b], Roma, Italy
L. Barone[a,b], F. Cavallari[a], M. Cipriani[a,b], G. D'imperio[a,b,15], D. Del Re[a,b,15], M. Diemoz[a], S. Gelli[a,b], C. Jorda[a], E. Longo[a,b], F. Margaroli[a,b], P. Meridiani[a], G. Organtini[a,b], R. Paramatti[a], F. Preiato[a,b], S. Rahatlou[a,b], C. Rovelli[a], F. Santanastasio[a,b]

INFN Sezione di Torino [a], Università di Torino [b], Torino, Italy, Università del Piemonte Orientale [c], Novara, Italy
N. Amapane[a,b], R. Arcidiacono[a,c,15], S. Argiro[a,b], M. Arneodo[a,c], N. Bartosik[a], R. Bellan[a,b], C. Biino[a], N. Cartiglia[a], F. Cenna[a,b], M. Costa[a,b], R. Covarelli[a,b], A. Degano[a,b], N. Demaria[a], L. Finco[a,b], B. Kiani[a,b], C. Mariotti[a], S. Maselli[a], E. Migliore[a,b], V. Monaco[a,b], E. Monteil[a,b], M.M. Obertino[a,b], L. Pacher[a,b], N. Pastrone[a], M. Pelliccioni[a], G.L. Pinna Angioni[a,b], F. Ravera[a,b], A. Romero[a,b], M. Ruspa[a,c], R. Sacchi[a,b], K. Shchelina[a,b], V. Sola[a], A. Solano[a,b], A. Staiano[a], P. Traczyk[a,b]

INFN Sezione di Trieste [a], Università di Trieste [b], Trieste, Italy
S. Belforte[a], M. Casarsa[a], F. Cossutti[a], G. Della Ricca[a,b], C. La Licata[a,b], A. Schizzi[a,b], A. Zanetti[a]

Kyungpook National University, Daegu, Korea
D.H. Kim, G.N. Kim, M.S. Kim, S. Lee, S.W. Lee, Y.D. Oh, S. Sekmen, D.C. Son, Y.C. Yang

Chonbuk National University, Jeonju, Korea
H. Kim, A. Lee

Hanyang University, Seoul, Korea
J.A. Brochero Cifuentes, T.J. Kim

Korea University, Seoul, Korea
S. Cho, S. Choi, Y. Go, D. Gyun, S. Ha, B. Hong, Y. Jo, Y. Kim, B. Lee, K. Lee, K.S. Lee, S. Lee, J. Lim, S.K. Park, Y. Roh

Seoul National University, Seoul, Korea
J. Almond, J. Kim, S.B. Oh, S.h. Seo, U.K. Yang, H.D. Yoo, G.B. Yu

University of Seoul, Seoul, Korea
M. Choi, H. Kim, H. Kim, J.H. Kim, J.S.H. Lee, I.C. Park, G. Ryu, M.S. Ryu

Sungkyunkwan University, Suwon, Korea
Y. Choi, J. Goh, C. Hwang, D. Kim, J. Lee, I. Yu

Vilnius University, Vilnius, Lithuania
V. Dudenas, A. Juodagalvis, J. Vaitkus

National Centre for Particle Physics, Universiti Malaya, Kuala Lumpur, Malaysia
I. Ahmed, Z.A. Ibrahim, J.R. Komaragiri, M.A.B. Md Ali[32], F. Mohamad Idris[33], W.A.T. Wan Abdullah, M.N. Yusli, Z. Zolkapli

Centro de Investigacion y de Estudios Avanzados del IPN, Mexico City, Mexico
H. Castilla-Valdez, E. De La Cruz-Burelo, I. Heredia-De La Cruz[34], A. Hernandez-Almada, R. Lopez-Fernandez, J. Mejia Guisao, A. Sanchez-Hernandez

Universidad Iberoamericana, Mexico City, Mexico
S. Carrillo Moreno, C. Oropeza Barrera, F. Vazquez Valencia

Benemerita Universidad Autonoma de Puebla, Puebla, Mexico
S. Carpinteyro, I. Pedraza, H.A. Salazar Ibarguen, C. Uribe Estrada

Universidad Autónoma de San Luis Potosí, San Luis Potosí, Mexico
A. Morelos Pineda

University of Auckland, Auckland, New Zealand
D. Krofcheck

University of Canterbury, Christchurch, New Zealand
P.H. Butler

National Centre for Physics, Quaid-I-Azam University, Islamabad, Pakistan
A. Ahmad, M. Ahmad, Q. Hassan, H.R. Hoorani, W.A. Khan, M.A. Shah, M. Shoaib, M. Waqas

National Centre for Nuclear Research, Swierk, Poland
H. Bialkowska, M. Bluj, B. Boimska, T. Frueboes, M. Górski, M. Kazana, K. Nawrocki, K. Romanowska-Rybinska, M. Szleper, P. Zalewski

Institute of Experimental Physics, Faculty of Physics, University of Warsaw, Warsaw, Poland
K. Bunkowski, A. Byszuk[35], K. Doroba, A. Kalinowski, M. Konecki, J. Krolikowski, M. Misiura, M. Olszewski, M. Walczak

Laboratório de Instrumentação e Física Experimental de Partículas, Lisboa, Portugal
P. Bargassa, C. Beirão Da Cruz E Silva, A. Di Francesco, P. Faccioli, P.G. Ferreira Parracho, M. Gallinaro, J. Hollar, N. Leonardo, L. Lloret Iglesias, M.V. Nemallapudi, J. Rodrigues Antunes, J. Seixas, O. Toldaiev, D. Vadruccio, J. Varela, P. Vischia

Joint Institute for Nuclear Research, Dubna, Russia
S. Afanasiev, P. Bunin, M. Gavrilenko, I. Golutvin, I. Gorbunov, A. Kamenev, V. Karjavin, A. Lanev, A. Malakhov, V. Matveev[36,37], P. Moisenz, V. Palichik, V. Perelygin, S. Shmatov, S. Shulha, N. Skatchkov, V. Smirnov, N. Voytishin, A. Zarubin

Petersburg Nuclear Physics Institute, Gatchina (St. Petersburg), Russia
L. Chtchipounov, V. Golovtsov, Y. Ivanov, V. Kim[38], E. Kuznetsova[39], V. Murzin, V. Oreshkin, V. Sulimov, A. Vorobyev

Institute for Nuclear Research, Moscow, Russia
Yu. Andreev, A. Dermenev, S. Gninenko, N. Golubev, A. Karneyeu, M. Kirsanov, N. Krasnikov, A. Pashenkov, D. Tlisov, A. Toropin

Institute for Theoretical and Experimental Physics, Moscow, Russia
V. Epshteyn, V. Gavrilov, N. Lychkovskaya, V. Popov, I. Pozdnyakov, G. Safronov, A. Spiridonov, M. Toms, E. Vlasov, A. Zhokin

National Research Nuclear University 'Moscow Engineering Physics Institute' (MEPhI), Moscow, Russia
M. Chadeeva[40], M. Danilov[40], O. Markin

P.N. Lebedev Physical Institute, Moscow, Russia
V. Andreev, M. Azarkin[37], I. Dremin[37], M. Kirakosyan, A. Leonidov[37], S.V. Rusakov, A. Terkulov

Skobeltsyn Institute of Nuclear Physics, Lomonosov Moscow State University, Moscow, Russia
A. Baskakov, A. Belyaev, E. Boos, M. Dubinin[41], L. Dudko, A. Ershov, A. Gribushin, V. Klyukhin, O. Kodolova, I. Lokhtin, I. Miagkov, S. Obraztsov, S. Petrushanko, V. Savrin, A. Snigirev

State Research Center of Russian Federation, Institute for High Energy Physics, Protvino, Russia
I. Azhgirey, I. Bayshev, S. Bitioukov, D. Elumakhov, V. Kachanov, A. Kalinin, D. Konstantinov, V. Krychkine, V. Petrov, R. Ryutin, A. Sobol, S. Troshin, N. Tyurin, A. Uzunian, A. Volkov

University of Belgrade, Faculty of Physics and Vinca Institute of Nuclear Sciences, Belgrade, Serbia
P. Adzic[42], P. Cirkovic, D. Devetak, J. Milosevic, V. Rekovic

Centro de Investigaciones Energéticas Medioambientales y Tecnológicas (CIEMAT), Madrid, Spain
J. Alcaraz Maestre, E. Calvo, M. Cerrada, M. Chamizo Llatas, N. Colino, B. De La Cruz, A. Delgado Peris, A. Escalante Del Valle, C. Fernandez Bedoya, J.P. Fernández Ramos, J. Flix, M.C. Fouz, P. Garcia-Abia, O. Gonzalez Lopez, S. Goy Lopez, J.M. Hernandez, M.I. Josa,

E. Navarro De Martino, A. Pérez-Calero Yzquierdo, J. Puerta Pelayo, A. Quintario Olmeda, I. Redondo, L. Romero, M.S. Soares

Universidad Autónoma de Madrid, Madrid, Spain
J.F. de Trocóniz, M. Missiroli, D. Moran

Universidad de Oviedo, Oviedo, Spain
J. Cuevas, J. Fernandez Menendez, I. Gonzalez Caballero, J.R. González Fernández, E. Palencia Cortezon, S. Sanchez Cruz, J.M. Vizan Garcia

Instituto de Física de Cantabria (IFCA), CSIC-Universidad de Cantabria, Santander, Spain
I.J. Cabrillo, A. Calderon, J.R. Castiñeiras De Saa, E. Curras, M. Fernandez, J. Garcia-Ferrero, G. Gomez, A. Lopez Virto, J. Marco, C. Martinez Rivero, F. Matorras, J. Piedra Gomez, T. Rodrigo, A. Ruiz-Jimeno, L. Scodellaro, N. Trevisani, I. Vila, R. Vilar Cortabitarte

CERN, European Organization for Nuclear Research, Geneva, Switzerland
D. Abbaneo, E. Auffray, G. Auzinger, M. Bachtis, P. Baillon, A.H. Ball, D. Barney, P. Bloch, A. Bocci, A. Bonato, C. Botta, T. Camporesi, R. Castello, M. Cepeda, G. Cerminara, M. D'Alfonso, D. d'Enterria, A. Dabrowski, V. Daponte, A. David, M. De Gruttola, F. De Guio, A. De Roeck, E. Di Marco[43], M. Dobson, M. Dordevic, B. Dorney, T. du Pree, D. Duggan, M. Dünser, N. Dupont, A. Elliott-Peisert, S. Fartoukh, G. Franzoni, J. Fulcher, W. Funk, D. Gigi, K. Gill, M. Girone, F. Glege, D. Gulhan, S. Gundacker, M. Guthoff, J. Hammer, P. Harris, J. Hegeman, V. Innocente, P. Janot, H. Kirschenmann, V. Knünz, A. Kornmayer[15], M.J. Kortelainen, K. Kousouris, M. Krammer[1], P. Lecoq, C. Lourenço, M.T. Lucchini, L. Malgeri, M. Mannelli, A. Martelli, F. Meijers, S. Mersi, E. Meschi, F. Moortgat, S. Morovic, M. Mulders, H. Neugebauer, S. Orfanelli[44], L. Orsini, L. Pape, E. Perez, M. Peruzzi, A. Petrilli, G. Petrucciani, A. Pfeiffer, M. Pierini, A. Racz, T. Reis, G. Rolandi[45], M. Rovere, M. Ruan, H. Sakulin, J.B. Sauvan, C. Schäfer, C. Schwick, M. Seidel, A. Sharma, P. Silva, M. Simon, P. Sphicas[46], J. Steggemann, M. Stoye, Y. Takahashi, M. Tosi, D. Treille, A. Triossi, A. Tsirou, V. Veckalns[47], G.I. Veres[21], N. Wardle, A. Zagozdzinska[35], W.D. Zeuner

Paul Scherrer Institut, Villigen, Switzerland
W. Bertl, K. Deiters, W. Erdmann, R. Horisberger, Q. Ingram, H.C. Kaestli, D. Kotlinski, U. Langenegger, T. Rohe

Institute for Particle Physics, ETH Zurich, Zurich, Switzerland
F. Bachmair, L. Bäni, L. Bianchini, B. Casal, G. Dissertori, M. Dittmar, M. Donegà, P. Eller, C. Grab, C. Heidegger, D. Hits, J. Hoss, G. Kasieczka, P. Lecomte†, W. Lustermann, B. Mangano, M. Marionneau, P. Martinez Ruiz del Arbol, M. Masciovecchio, M.T. Meinhard, D. Meister, F. Micheli, P. Musella, F. Nessi-Tedaldi, F. Pandolfi, J. Pata, F. Pauss, G. Perrin, L. Perrozzi, M. Quittnat, M. Rossini, M. Schönenberger, A. Starodumov[48], M. Takahashi, V.R. Tavolaro, K. Theofilatos, R. Wallny

Universität Zürich, Zurich, Switzerland
T.K. Aarrestad, C. Amsler[49], L. Caminada, M.F. Canelli, V. Chiochia, A. De Cosa, C. Galloni, A. Hinzmann, T. Hreus, B. Kilminster, C. Lange, J. Ngadiuba, D. Pinna, G. Rauco, P. Robmann, D. Salerno, Y. Yang

National Central University, Chung-Li, Taiwan
V. Candelise, T.H. Doan, Sh. Jain, R. Khurana, M. Konyushikhin, C.M. Kuo, W. Lin, Y.J. Lu, A. Pozdnyakov, S.S. Yu

National Taiwan University (NTU), Taipei, Taiwan
Arun Kumar, P. Chang, Y.H. Chang, Y.W. Chang, Y. Chao, K.F. Chen, P.H. Chen, C. Dietz,

F. Fiori, W.-S. Hou, Y. Hsiung, Y.F. Liu, R.-S. Lu, M. Miñano Moya, E. Paganis, A. Psallidas, J.f. Tsai, Y.M. Tzeng

Chulalongkorn University, Faculty of Science, Department of Physics, Bangkok, Thailand
B. Asavapibhop, G. Singh, N. Srimanobhas, N. Suwonjandee

Cukurova University, Adana, Turkey
A. Adiguzel, S. Cerci[50], S. Damarseckin, Z.S. Demiroglu, C. Dozen, I. Dumanoglu, S. Girgis, G. Gokbulut, Y. Guler, E. Gurpinar, I. Hos, E.E. Kangal[51], O. Kara, A. Kayis Topaksu, U. Kiminsu, M. Oglakci, G. Onengut[52], K. Ozdemir[53], D. Sunar Cerci[50], H. Topakli[54], S. Turkcapar, I.S. Zorbakir, C. Zorbilmez

Middle East Technical University, Physics Department, Ankara, Turkey
B. Bilin, S. Bilmis, B. Isildak[55], G. Karapinar[56], M. Yalvac, M. Zeyrek

Bogazici University, Istanbul, Turkey
E. Gülmez, M. Kaya[57], O. Kaya[58], E.A. Yetkin[59], T. Yetkin[60]

Istanbul Technical University, Istanbul, Turkey
A. Cakir, K. Cankocak, S. Sen[61]

Institute for Scintillation Materials of National Academy of Science of Ukraine, Kharkov, Ukraine
B. Grynyov

National Scientific Center, Kharkov Institute of Physics and Technology, Kharkov, Ukraine
L. Levchuk, P. Sorokin

University of Bristol, Bristol, United Kingdom
R. Aggleton, F. Ball, L. Beck, J.J. Brooke, D. Burns, E. Clement, D. Cussans, H. Flacher, J. Goldstein, M. Grimes, G.P. Heath, H.F. Heath, J. Jacob, L. Kreczko, C. Lucas, D.M. Newbold[62], S. Paramesvaran, A. Poll, T. Sakuma, S. Seif El Nasr-storey, D. Smith, V.J. Smith

Rutherford Appleton Laboratory, Didcot, United Kingdom
K.W. Bell, A. Belyaev[63], C. Brew, R.M. Brown, L. Calligaris, D. Cieri, D.J.A. Cockerill, J.A. Coughlan, K. Harder, S. Harper, E. Olaiya, D. Petyt, C.H. Shepherd-Themistocleous, A. Thea, I.R. Tomalin, T. Williams

Imperial College, London, United Kingdom
M. Baber, R. Bainbridge, O. Buchmuller, A. Bundock, D. Burton, S. Casasso, M. Citron, D. Colling, L. Corpe, P. Dauncey, G. Davies, A. De Wit, M. Della Negra, P. Dunne, A. Elwood, D. Futyan, Y. Haddad, G. Hall, G. Iles, R. Lane, C. Laner, R. Lucas[62], L. Lyons, A.-M. Magnan, S. Malik, L. Mastrolorenzo, J. Nash, A. Nikitenko[48], J. Pela, B. Penning, M. Pesaresi, D.M. Raymond, A. Richards, A. Rose, C. Seez, A. Tapper, K. Uchida, M. Vazquez Acosta[64], T. Virdee[15], S.C. Zenz

Brunel University, Uxbridge, United Kingdom
J.E. Cole, P.R. Hobson, A. Khan, P. Kyberd, D. Leslie, I.D. Reid, P. Symonds, L. Teodorescu, M. Turner

Baylor University, Waco, USA
A. Borzou, K. Call, J. Dittmann, K. Hatakeyama, H. Liu, N. Pastika

The University of Alabama, Tuscaloosa, USA
O. Charaf, S.I. Cooper, C. Henderson, P. Rumerio

Boston University, Boston, USA
D. Arcaro, A. Avetisyan, T. Bose, D. Gastler, D. Rankin, C. Richardson, J. Rohlf, L. Sulak, D. Zou

Brown University, Providence, USA
G. Benelli, E. Berry, D. Cutts, A. Garabedian, J. Hakala, U. Heintz, O. Jesus, E. Laird, G. Landsberg, Z. Mao, M. Narain, S. Piperov, S. Sagir, E. Spencer, R. Syarif

University of California, Davis, Davis, USA
R. Breedon, G. Breto, D. Burns, M. Calderon De La Barca Sanchez, S. Chauhan, M. Chertok, J. Conway, R. Conway, P.T. Cox, R. Erbacher, C. Flores, G. Funk, M. Gardner, W. Ko, R. Lander, C. Mclean, M. Mulhearn, D. Pellett, J. Pilot, F. Ricci-Tam, S. Shalhout, J. Smith, M. Squires, D. Stolp, M. Tripathi, S. Wilbur, R. Yohay

University of California, Los Angeles, USA
R. Cousins, P. Everaerts, A. Florent, J. Hauser, M. Ignatenko, D. Saltzberg, E. Takasugi, V. Valuev, M. Weber

University of California, Riverside, Riverside, USA
K. Burt, R. Clare, J. Ellison, J.W. Gary, G. Hanson, J. Heilman, P. Jandir, E. Kennedy, F. Lacroix, O.R. Long, M. Malberti, M. Olmedo Negrete, M.I. Paneva, A. Shrinivas, H. Wei, S. Wimpenny, B. R. Yates

University of California, San Diego, La Jolla, USA
J.G. Branson, G.B. Cerati, S. Cittolin, M. Derdzinski, R. Gerosa, A. Holzner, D. Klein, J. Letts, I. Macneill, D. Olivito, S. Padhi, M. Pieri, M. Sani, V. Sharma, S. Simon, M. Tadel, A. Vartak, S. Wasserbaech[65], C. Welke, J. Wood, F. Würthwein, A. Yagil, G. Zevi Della Porta

University of California, Santa Barbara, Santa Barbara, USA
R. Bhandari, J. Bradmiller-Feld, C. Campagnari, A. Dishaw, V. Dutta, K. Flowers, M. Franco Sevilla, P. Geffert, C. George, F. Golf, L. Gouskos, J. Gran, R. Heller, J. Incandela, N. Mccoll, S.D. Mullin, A. Ovcharova, J. Richman, D. Stuart, I. Suarez, C. West, J. Yoo

California Institute of Technology, Pasadena, USA
D. Anderson, A. Apresyan, J. Bendavid, A. Bornheim, J. Bunn, Y. Chen, J. Duarte, A. Mott, H.B. Newman, C. Pena, M. Spiropulu, J.R. Vlimant, S. Xie, R.Y. Zhu

Carnegie Mellon University, Pittsburgh, USA
M.B. Andrews, V. Azzolini, B. Carlson, T. Ferguson, M. Paulini, J. Russ, M. Sun, H. Vogel, I. Vorobiev

University of Colorado Boulder, Boulder, USA
J.P. Cumalat, W.T. Ford, F. Jensen, A. Johnson, M. Krohn, T. Mulholland, K. Stenson, S.R. Wagner

Cornell University, Ithaca, USA
J. Alexander, J. Chaves, J. Chu, S. Dittmer, K. Mcdermott, N. Mirman, G. Nicolas Kaufman, J.R. Patterson, A. Rinkevicius, A. Ryd, L. Skinnari, L. Soffi, S.M. Tan, Z. Tao, J. Thom, J. Tucker, P. Wittich, M. Zientek

Fairfield University, Fairfield, USA
D. Winn

Fermi National Accelerator Laboratory, Batavia, USA
S. Abdullin, M. Albrow, G. Apollinari, S. Banerjee, L.A.T. Bauerdick, A. Beretvas, J. Berryhill, P.C. Bhat, G. Bolla, K. Burkett, J.N. Butler, H.W.K. Cheung, F. Chlebana, S. Cihangir,

M. Cremonesi, V.D. Elvira, I. Fisk, J. Freeman, E. Gottschalk, L. Gray, D. Green, S. Grünendahl, O. Gutsche, D. Hare, R.M. Harris, S. Hasegawa, J. Hirschauer, Z. Hu, B. Jayatilaka, S. Jindariani, M. Johnson, U. Joshi, B. Klima, B. Kreis, S. Lammel, J. Linacre, D. Lincoln, R. Lipton, T. Liu, R. Lopes De Sá, J. Lykken, K. Maeshima, N. Magini, J.M. Marraffino, S. Maruyama, D. Mason, P. McBride, P. Merkel, S. Mrenna, S. Nahn, C. Newman-Holmes†, V. O'Dell, K. Pedro, O. Prokofyev, G. Rakness, L. Ristori, E. Sexton-Kennedy, A. Soha, W.J. Spalding, L. Spiegel, S. Stoynev, N. Strobbe, L. Taylor, S. Tkaczyk, N.V. Tran, L. Uplegger, E.W. Vaandering, C. Vernieri, M. Verzocchi, R. Vidal, M. Wang, H.A. Weber, A. Whitbeck

University of Florida, Gainesville, USA
D. Acosta, P. Avery, P. Bortignon, D. Bourilkov, A. Brinkerhoff, A. Carnes, M. Carver, D. Curry, S. Das, R.D. Field, I.K. Furic, J. Konigsberg, A. Korytov, P. Ma, K. Matchev, H. Mei, P. Milenovic[66], G. Mitselmakher, D. Rank, L. Shchutska, D. Sperka, L. Thomas, J. Wang, S. Wang, J. Yelton

Florida International University, Miami, USA
S. Linn, P. Markowitz, G. Martinez, J.L. Rodriguez

Florida State University, Tallahassee, USA
A. Ackert, J.R. Adams, T. Adams, A. Askew, S. Bein, B. Diamond, S. Hagopian, V. Hagopian, K.F. Johnson, A. Khatiwada, H. Prosper, A. Santra, M. Weinberg

Florida Institute of Technology, Melbourne, USA
M.M. Baarmand, V. Bhopatkar, S. Colafranceschi[67], M. Hohlmann, D. Noonan, T. Roy, F. Yumiceva

University of Illinois at Chicago (UIC), Chicago, USA
M.R. Adams, L. Apanasevich, D. Berry, R.R. Betts, I. Bucinskaite, R. Cavanaugh, O. Evdokimov, L. Gauthier, C.E. Gerber, D.J. Hofman, P. Kurt, C. O'Brien, I.D. Sandoval Gonzalez, P. Turner, N. Varelas, Z. Wu, M. Zakaria, J. Zhang

The University of Iowa, Iowa City, USA
B. Bilki[68], W. Clarida, K. Dilsiz, S. Durgut, R.P. Gandrajula, M. Haytmyradov, V. Khristenko, J.-P. Merlo, H. Mermerkaya[69], A. Mestvirishvili, A. Moeller, J. Nachtman, H. Ogul, Y. Onel, F. Ozok[70], A. Penzo, C. Snyder, E. Tiras, J. Wetzel, K. Yi

Johns Hopkins University, Baltimore, USA
I. Anderson, B. Blumenfeld, A. Cocoros, N. Eminizer, D. Fehling, L. Feng, A.V. Gritsan, P. Maksimovic, M. Osherson, J. Roskes, U. Sarica, M. Swartz, M. Xiao, Y. Xin, C. You

The University of Kansas, Lawrence, USA
A. Al-bataineh, P. Baringer, A. Bean, J. Bowen, C. Bruner, J. Castle, R.P. Kenny III, A. Kropivnitskaya, D. Majumder, W. Mcbrayer, M. Murray, S. Sanders, R. Stringer, J.D. Tapia Takaki, Q. Wang

Kansas State University, Manhattan, USA
A. Ivanov, K. Kaadze, S. Khalil, M. Makouski, Y. Maravin, A. Mohammadi, L.K. Saini, N. Skhirtladze, S. Toda

Lawrence Livermore National Laboratory, Livermore, USA
D. Lange, F. Rebassoo, D. Wright

University of Maryland, College Park, USA
C. Anelli, A. Baden, O. Baron, A. Belloni, B. Calvert, S.C. Eno, C. Ferraioli, J.A. Gomez,

N.J. Hadley, S. Jabeen, R.G. Kellogg, T. Kolberg, J. Kunkle, Y. Lu, A.C. Mignerey, Y.H. Shin, A. Skuja, M.B. Tonjes, S.C. Tonwar

Massachusetts Institute of Technology, Cambridge, USA
D. Abercrombie, B. Allen, A. Apyan, R. Barbieri, A. Baty, R. Bi, K. Bierwagen, S. Brandt, W. Busza, I.A. Cali, Z. Demiragli, L. Di Matteo, G. Gomez Ceballos, M. Goncharov, D. Hsu, Y. Iiyama, G.M. Innocenti, M. Klute, D. Kovalskyi, K. Krajczar, Y.S. Lai, Y.-J. Lee, A. Levin, P.D. Luckey, A.C. Marini, C. Mcginn, C. Mironov, S. Narayanan, X. Niu, C. Paus, C. Roland, G. Roland, J. Salfeld-Nebgen, G.S.F. Stephans, K. Sumorok, K. Tatar, M. Varma, D. Velicanu, J. Veverka, J. Wang, T.W. Wang, B. Wyslouch, M. Yang, V. Zhukova

University of Minnesota, Minneapolis, USA
A.C. Benvenuti, R.M. Chatterjee, A. Evans, A. Finkel, A. Gude, P. Hansen, S. Kalafut, S.C. Kao, Y. Kubota, Z. Lesko, J. Mans, S. Nourbakhsh, N. Ruckstuhl, R. Rusack, N. Tambe, J. Turkewitz

University of Mississippi, Oxford, USA
J.G. Acosta, S. Oliveros

University of Nebraska-Lincoln, Lincoln, USA
E. Avdeeva, R. Bartek, K. Bloom, S. Bose, D.R. Claes, A. Dominguez, C. Fangmeier, R. Gonzalez Suarez, R. Kamalieddin, D. Knowlton, I. Kravchenko, A. Malta Rodrigues, F. Meier, J. Monroy, J.E. Siado, G.R. Snow, B. Stieger

State University of New York at Buffalo, Buffalo, USA
M. Alyari, J. Dolen, J. George, A. Godshalk, C. Harrington, I. Iashvili, J. Kaisen, A. Kharchilava, A. Kumar, A. Parker, S. Rappoccio, B. Roozbahani

Northeastern University, Boston, USA
G. Alverson, E. Barberis, D. Baumgartel, M. Chasco, A. Hortiangtham, A. Massironi, D.M. Morse, D. Nash, T. Orimoto, R. Teixeira De Lima, D. Trocino, R.-J. Wang, D. Wood

Northwestern University, Evanston, USA
S. Bhattacharya, K.A. Hahn, A. Kubik, J.F. Low, N. Mucia, N. Odell, B. Pollack, M.H. Schmitt, K. Sung, M. Trovato, M. Velasco

University of Notre Dame, Notre Dame, USA
N. Dev, M. Hildreth, K. Hurtado Anampa, C. Jessop, D.J. Karmgard, N. Kellams, K. Lannon, N. Marinelli, F. Meng, C. Mueller, Y. Musienko[36], M. Planer, A. Reinsvold, R. Ruchti, G. Smith, S. Taroni, N. Valls, M. Wayne, M. Wolf, A. Woodard

The Ohio State University, Columbus, USA
J. Alimena, L. Antonelli, J. Brinson, B. Bylsma, L.S. Durkin, S. Flowers, B. Francis, A. Hart, C. Hill, R. Hughes, W. Ji, B. Liu, W. Luo, D. Puigh, B.L. Winer, H.W. Wulsin

Princeton University, Princeton, USA
S. Cooperstein, O. Driga, P. Elmer, J. Hardenbrook, P. Hebda, J. Luo, D. Marlow, T. Medvedeva, M. Mooney, J. Olsen, C. Palmer, P. Piroué, D. Stickland, C. Tully, A. Zuranski

University of Puerto Rico, Mayaguez, USA
S. Malik

Purdue University, West Lafayette, USA
A. Barker, V.E. Barnes, D. Benedetti, S. Folgueras, L. Gutay, M.K. Jha, M. Jones, A.W. Jung, K. Jung, D.H. Miller, N. Neumeister, B.C. Radburn-Smith, X. Shi, J. Sun, A. Svyatkovskiy, F. Wang, W. Xie, L. Xu

Purdue University Calumet, Hammond, USA
N. Parashar, J. Stupak

Rice University, Houston, USA
A. Adair, B. Akgun, Z. Chen, K.M. Ecklund, F.J.M. Geurts, M. Guilbaud, W. Li, B. Michlin, M. Northup, B.P. Padley, R. Redjimi, J. Roberts, J. Rorie, Z. Tu, J. Zabel

University of Rochester, Rochester, USA
B. Betchart, A. Bodek, P. de Barbaro, R. Demina, Y.t. Duh, T. Ferbel, M. Galanti, A. Garcia-Bellido, J. Han, O. Hindrichs, A. Khukhunaishvili, K.H. Lo, P. Tan, M. Verzetti

Rutgers, The State University of New Jersey, Piscataway, USA
J.P. Chou, E. Contreras-Campana, Y. Gershtein, T.A. Gómez Espinosa, E. Halkiadakis, M. Heindl, D. Hidas, E. Hughes, S. Kaplan, R. Kunnawalkam Elayavalli, S. Kyriacou, A. Lath, K. Nash, H. Saka, S. Salur, S. Schnetzer, D. Sheffield, S. Somalwar, R. Stone, S. Thomas, P. Thomassen, M. Walker

University of Tennessee, Knoxville, USA
M. Foerster, J. Heideman, G. Riley, K. Rose, S. Spanier, K. Thapa

Texas A&M University, College Station, USA
O. Bouhali[71], A. Celik, M. Dalchenko, M. De Mattia, A. Delgado, S. Dildick, R. Eusebi, J. Gilmore, T. Huang, E. Juska, T. Kamon[72], V. Krutelyov, R. Mueller, Y. Pakhotin, R. Patel, A. Perloff, L. Perniè, D. Rathjens, A. Rose, A. Safonov, A. Tatarinov, K.A. Ulmer

Texas Tech University, Lubbock, USA
N. Akchurin, C. Cowden, J. Damgov, C. Dragoiu, P.R. Dudero, J. Faulkner, S. Kunori, K. Lamichhane, S.W. Lee, T. Libeiro, S. Undleeb, I. Volobouev, Z. Wang

Vanderbilt University, Nashville, USA
A.G. Delannoy, S. Greene, A. Gurrola, R. Janjam, W. Johns, C. Maguire, A. Melo, H. Ni, P. Sheldon, S. Tuo, J. Velkovska, Q. Xu

University of Virginia, Charlottesville, USA
M.W. Arenton, P. Barria, B. Cox, J. Goodell, R. Hirosky, A. Ledovskoy, H. Li, C. Neu, T. Sinthuprasith, X. Sun, Y. Wang, E. Wolfe, F. Xia

Wayne State University, Detroit, USA
C. Clarke, R. Harr, P.E. Karchin, P. Lamichhane, J. Sturdy

University of Wisconsin - Madison, Madison, WI, USA
D.A. Belknap, S. Dasu, L. Dodd, S. Duric, B. Gomber, M. Grothe, M. Herndon, A. Hervé, P. Klabbers, A. Lanaro, A. Levine, K. Long, R. Loveless, I. Ojalvo, T. Perry, G.A. Pierro, G. Polese, T. Ruggles, A. Savin, A. Sharma, N. Smith, W.H. Smith, D. Taylor, N. Woods

†: Deceased
1: Also at Vienna University of Technology, Vienna, Austria
2: Also at State Key Laboratory of Nuclear Physics and Technology, Peking University, Beijing, China
3: Also at Institut Pluridisciplinaire Hubert Curien, Université de Strasbourg, Université de Haute Alsace Mulhouse, CNRS/IN2P3, Strasbourg, France
4: Also at Universidade Estadual de Campinas, Campinas, Brazil
5: Also at Centre National de la Recherche Scientifique (CNRS) - IN2P3, Paris, France
6: Also at Université Libre de Bruxelles, Bruxelles, Belgium
7: Also at Deutsches Elektronen-Synchrotron, Hamburg, Germany

8: Also at Joint Institute for Nuclear Research, Dubna, Russia
9: Also at Helwan University, Cairo, Egypt
10: Now at Zewail City of Science and Technology, Zewail, Egypt
11: Also at Ain Shams University, Cairo, Egypt
12: Also at Fayoum University, El-Fayoum, Egypt
13: Now at British University in Egypt, Cairo, Egypt
14: Also at Université de Haute Alsace, Mulhouse, France
15: Also at CERN, European Organization for Nuclear Research, Geneva, Switzerland
16: Also at Skobeltsyn Institute of Nuclear Physics, Lomonosov Moscow State University, Moscow, Russia
17: Also at RWTH Aachen University, III. Physikalisches Institut A, Aachen, Germany
18: Also at University of Hamburg, Hamburg, Germany
19: Also at Brandenburg University of Technology, Cottbus, Germany
20: Also at Institute of Nuclear Research ATOMKI, Debrecen, Hungary
21: Also at MTA-ELTE Lendület CMS Particle and Nuclear Physics Group, Eötvös Loránd University, Budapest, Hungary
22: Also at University of Debrecen, Debrecen, Hungary
23: Also at Indian Institute of Science Education and Research, Bhopal, India
24: Also at Institute of Physics, Bhubaneswar, India
25: Also at University of Visva-Bharati, Santiniketan, India
26: Also at University of Ruhuna, Matara, Sri Lanka
27: Also at Isfahan University of Technology, Isfahan, Iran
28: Also at University of Tehran, Department of Engineering Science, Tehran, Iran
29: Also at Plasma Physics Research Center, Science and Research Branch, Islamic Azad University, Tehran, Iran
30: Also at Università degli Studi di Siena, Siena, Italy
31: Also at Purdue University, West Lafayette, USA
32: Also at International Islamic University of Malaysia, Kuala Lumpur, Malaysia
33: Also at Malaysian Nuclear Agency, MOSTI, Kajang, Malaysia
34: Also at Consejo Nacional de Ciencia y Tecnología, Mexico city, Mexico
35: Also at Warsaw University of Technology, Institute of Electronic Systems, Warsaw, Poland
36: Also at Institute for Nuclear Research, Moscow, Russia
37: Now at National Research Nuclear University 'Moscow Engineering Physics Institute' (MEPhI), Moscow, Russia
38: Also at St. Petersburg State Polytechnical University, St. Petersburg, Russia
39: Also at University of Florida, Gainesville, USA
40: Also at P.N. Lebedev Physical Institute, Moscow, Russia
41: Also at California Institute of Technology, Pasadena, USA
42: Also at Faculty of Physics, University of Belgrade, Belgrade, Serbia
43: Also at INFN Sezione di Roma; Università di Roma, Roma, Italy
44: Also at National Technical University of Athens, Athens, Greece
45: Also at Scuola Normale e Sezione dell'INFN, Pisa, Italy
46: Also at National and Kapodistrian University of Athens, Athens, Greece
47: Also at Riga Technical University, Riga, Latvia
48: Also at Institute for Theoretical and Experimental Physics, Moscow, Russia
49: Also at Albert Einstein Center for Fundamental Physics, Bern, Switzerland
50: Also at Adiyaman University, Adiyaman, Turkey
51: Also at Mersin University, Mersin, Turkey
52: Also at Cag University, Mersin, Turkey

53: Also at Piri Reis University, Istanbul, Turkey
54: Also at Gaziosmanpasa University, Tokat, Turkey
55: Also at Ozyegin University, Istanbul, Turkey
56: Also at Izmir Institute of Technology, Izmir, Turkey
57: Also at Marmara University, Istanbul, Turkey
58: Also at Kafkas University, Kars, Turkey
59: Also at Istanbul Bilgi University, Istanbul, Turkey
60: Also at Yildiz Technical University, Istanbul, Turkey
61: Also at Hacettepe University, Ankara, Turkey
62: Also at Rutherford Appleton Laboratory, Didcot, United Kingdom
63: Also at School of Physics and Astronomy, University of Southampton, Southampton, United Kingdom
64: Also at Instituto de Astrofísica de Canarias, La Laguna, Spain
65: Also at Utah Valley University, Orem, USA
66: Also at University of Belgrade, Faculty of Physics and Vinca Institute of Nuclear Sciences, Belgrade, Serbia
67: Also at Facoltà Ingegneria, Università di Roma, Roma, Italy
68: Also at Argonne National Laboratory, Argonne, USA
69: Also at Erzincan University, Erzincan, Turkey
70: Also at Mimar Sinan University, Istanbul, Istanbul, Turkey
71: Also at Texas A&M University at Qatar, Doha, Qatar
72: Also at Kyungpook National University, Daegu, Korea